RoJAE

Romanian Journal of Automotive Engineering

SIAR

The Journal of the Society of Automotive Engineers of Romania
www.siar.ro
www.ro-jae.ro

RoJAE
Romanian
Journal of Automotive Engineering

SIAR – The Society of Automotive Engineers of Romania is the professional organization of automotive engineers, an independent legal entity, non-profit, active member of FISITA (Fédération Internationale des Sociétés d'Ingénieurs des Techniques de l'Automobile - International Federation of Automotive Engineering Societies) and EAEC (European Cooperation Automotive Engineers).

Founded in January 1990 as a professional association, non-governmental, SIAR's main objectives are: development and increase the exchange of professional information, promoting Romanian scientific research results, new technologies specific to automotive industry, international cooperation.

Shortly after its constitution, SIAR was affiliated to FISITA - International Federation of Automotive Engineers and EAEC - European Conference of Automotive Engineers, thus ensuring full involvement in specific activities undertaken globally.

In order to help promoting the science and technology in the automotive industry, SIAR is issuing 4 times a year rIA - Journal of Automotive Engineers (on paper in Romanian and electronically in Romanian and English).

The organization of national and international scientific meetings with a large participation of experts from universities and research institutes and economic environment is an important part of SIAR's. In this direction, SIAR holds an annual scientific event with a wide international participation. The SIAR annual congress is hosted successively by large universities that have ongoing programs of study in automotive engineering.

Developing relationships with the economic environment is a constant concern. The presence in Romania of OEMs and their suppliers enables continuous communication between industry and academia.

A constant priority in SIAR's activity is to ensure optimal framework for collaboration between universities and research, industry and business specialists.

CONTENTS

Volume 27, Issue No. 3   **September 2021**

The RoJAE's articles are included in the *„Ingineria automobilului"* magazine (*ISSN 1842 – 4074*), published by SIAR in Romanian.

The articles published in *„Ingineria automobilului"* magazine are indexed by Web of Science in the *„Emerging Source Citation Index (ESCI)"* Section.

Web of Science

Clarivate Analytics

THE USE OF NATURAL GAS MIXED WITH HYDROGEN AS FUEL FOR SPARK-IGNITION ENGINES

Marius Cătălin BARBU[*], Radu CHIRIAC

Politehnica University of Bucharest, Faculty of Mechanical Engineering and Mechatronics,
Splaiul Independenței 313, 060042 BUCHAREST, Romania

Abstract: *This paper presents the current situation regarding the development of the supply infrastructure of compressed natural gas (CNG) and liquefied natural gas (LNG) as well as the supply systems of vehicles with these alternative fuels. The results of experimental studies on the use of natural gas mixed with hydrogen as a fuel for spark-ignition engines are highlighted, considering current legislation on pollutant emissions. The results show the advantages in terms of combustion process and combustion velocity in the spark ignited engine fueled with natural gas improved by mixing with hydrogen. Emissions of hydrocarbons (HC), carbon dioxide (CO2), and carbon monoxide (CO) decrease with the increasing percentage of hydrogen. Normally the nitrogen oxide emissions (NOx) increase with the increasing of hydrogen fraction in mixed fuel due to higher temperatures of cylinder charge. Hydrogen enrichment extends the combustion limit of compressed hydrogen-natural gas (HGNC) mixtures. The addition of hydrogen (H2) in volumetric fractions of 20-30% in natural gas can be an effective short-term solution to the globally huge problem of greenhouse gases, without requiring significant changes to current technologies used in engines. To obtain significantly improved performance characteristics, the compression ratio of the engine can be increased when using CNG mixed with H2 due to the higher-octane number than for petrol.*

Keywords*: CNG, Hydrogen, Emissions, Spark-ignition Engine*

1. INTRODUCTION

With increasingly stringent pollution rules demands, carmakers are trying to adapt alternative propulsion solutions using new energy sources other than fossil fuels. One alternative is compressed natural gas (CNG), which is natural gas stored in pressure vessel tanks (200-250 bar) for use as fuel for heat engine vehicles. Another alternative solution is hydrogen (H_2) which is a tasteless, colorless, and odorless gas. This gas does not include carbon atoms in its molecule; after combustion (oxidation), no polluting gases such as carbon dioxide (CO_2), hydrocarbons (HC) and carbon monoxide (CO) results. The mixture of hydrogen and natural gas in different fractions called HCNG (Hydrogen-Natural Gas Mixture) can be considered a motor fuel, without requiring major changes to the internal combustion engine. The benefits of these fuels would be that they are less polluting, renewable, and more economically viable than petrol.

2. FUELS AND PROPERTIES

2.1 Fuel classification
Conventional fuels used in internal combustion engines are petroleum in nature, derived from chemical combinations of carbon and hydrogen (hydrocarbons). Unconventional fuels are other than oil, like synthetic or natural, in liquid, gaseous, or even solid-state.
Alternatives to petrol and diesel can be unconventional fuels. Of these fuels, it is estimated that hydrogen has the most open future for powering heat engines, arguing that current engines, both spark-ignition engines and Diesel engine, can be adapted for hydrogen operation.
Hydrogen offers a mass calorific value of 121,126 kJ/kg, so 2.8 times higher than gasoline.
The ignition energy is 15 times lower, and the maximum flame propagation speed is 8 times higher, and the hydrogen vapors are not toxic [1].

---

[*] *Corresponding author e-mail: marius.barbu91@yahoo.ro*

The expansion of the use of hydrogen in heat engines is slowed down by the high cost of the unit mass (volume) of liquid H_2.

The density and calorific value of the volume (12250 kJ/m3N) are lower than those of petrol and diesel and the high combustion rate, the rapid propagation of the flame, the reverse explosions in the intake pipe must be considered when using hydrogen.

There are prospects for the production and storage of H_2 in optimal conditions.

2.2 Compressed natural gas

Methane can be compressed and stored in metal tanks at pressures of 200-250 bar under the name of Compressed Natural Gas (CNG) or liquefied at - 163˚C and stored under the name of Liquefied Natural Gas (LNG).

Unlike traditional fuels, gasoline, and diesel, CNG has the following advantages:
•   It is about 40% cheaper
•   CNG combustion emits 30% less CO_2 emissions.
•   It is non-toxic and disperses quickly
•   Safer technology with lighter composite cylinders.

Biogas is a renewable resource that is obtained from waste agricultural materials (plants or animals) from wastewater purification processes, from municipal waste, from wood and crop plants. Biogas is usually used to power the engines of electric generators, but, improved as Biomethane can be used to power vehicles.

The typical physicochemical properties of some relevant fuels are presented in table 1:

Table 1.
Typical physicochemical properties of relevant fuels [2]

Properties	Methane	Hydrogen	Gasoline	Diesel
Molar mass [kg/mol]	16,04	2,02	100-108	204
Laminar flame speed at NTP [m/s]	0,38	2,65-3,25	0,37-0,43	-
Minimum ignition energy [mJ]	0,28	0,02	0,25	-
Adiabatic flame temperature in NTP air [K]	2224	2379	2470	2327
Quenching distance in NTP air [mm]	2,03	0,64	2	-
Density at NTP [kg/m³]	0,67	0,08	720-775	833-881
Flammability limits in air (vol%) [lower–upper]	5,3-15,0	4,0-75,0	1,2-6,0	0,7-5
Lower heating value	46,72	119,7	44,79	42,5
Diffusion coefficient [cm²/s]	0,189	0,61	-	-
LHV of stoichiometric mixture [MJ/m³]	3,13	3,02	3,83	-
Auto-ignition temperature in air [K]	813	858	500-750	553
Volumetric LHV [MJ/m³]	32,97	10,22	216,38	-

2.3 Hydrogen methane mixture

The figure 1 below shows the evolution of alternative fuel consumption in the coming years. Alternative fuel is known to emit fewer pollutant emissions than gasoline. This renewable fuel is obtained from sources other than petroleum, in addition, it is more economically viable [4].

An increase in turbulence in the cylinder is used to increase the flame velocity of lean mixtures of natural gas as well as to increase the flammability limits.

Turbulence will increase the heat transfer to the walls but will also increase the combustion temperatures which will lead to higher NOx emissions [4].

Hydrogen is a fuel that burns at high speed and with lean air-fuel mixtures.

That is why hydrogen can be used in combination with CNG to improve the low burning speed of natural gas and to increase its ignition limit.
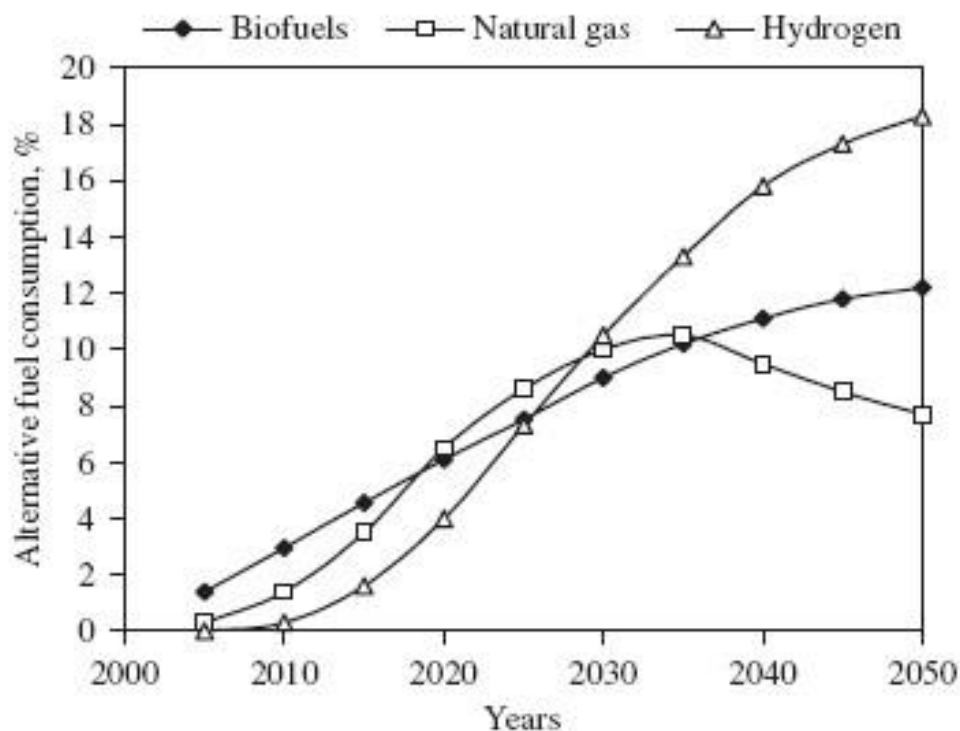
Figure 1. Alternative fuels consumption worldwide [4]

Also, the addition of hydrogen will reduce engine emissions [5][6].
A mixture of 7% by energy between hydrogen and CNG is obtained with 20% (by volume) of hydrogen in CNG (or 3% by mass).
In table 2 are presented the properties of gasoline, hydrogen, CNG and 5% by energy HCNG [7].

Table 2.
Properties of petrol, CNG, 5% energy HCNG and hydrogen [7]

Properties	Gasoline	H2	CNG	HCNG
Diffusivity in air [$cm^2\ s^{-1}$]	0.08	0.63	0.2	0.31
Normalized flame emissivity	1.7	1.00	1.7	1.5
Burning velocity in NTP air [$cm\ s^{-1}$]	37-43	325	45	110
Minimum energy for ignition in air [mJ]	0.24	0.02	0.29	0.21
Quenching gap in NTP air [cm]	0.2	0.064	0.203	0.152
Percentage of radiated thermal energy	30-42	17-25	23-33	20-28
Equivalence ratio	0.7-3.8	0.1-7.1	0.7-4	0.5-5.4
Limits of flammability in air [vol %]	1.0-7.6	4-75	5-15	5-35
Auto ignition temp. [K]	501-744	858	813	825
Flame temp in air [K]	2470	2318	2148	2210
Stoichiometric volume fraction in air [vol %]	1.76	29.53	9.43	22.8

Several researchers have conducted tests on spark-ignition engines with various blends of HCNG.
The combustion of hydrogen, natural gas and their mixtures have been studied mainly.
Hydrogen and CNG storage are a challenge for researchers that is been considered.
A review of HCNG mixtures was performed to understand the effect of CNG enriched with hydrogen on spark-ignition engines.
The characteristics of the combustion of HCNG largely depend on the engine operating conditions.

Air-fuel ratio, injection timing, engine speed and compression ratio play a major role in mixing HCNG on engines.

The advantages of HCNG are:
- Higher burning speed
- Improved combustion of lean mixtures due to the wide flammability limit of hydrogen
- Reduction of certain pollutant emissions directly proportional to the amount of hydrogen
- Easy mixing due to gaseous conditions

3. INFRASTRUCTURE DEVELOPMENT

The following figure 2 shows a continuous growth in recent years which marks a development of the refueling infrastructure in Europe and the European Free Trade Association (EFTA) that encourage the industrial sectors associated with these gaseous fuels.
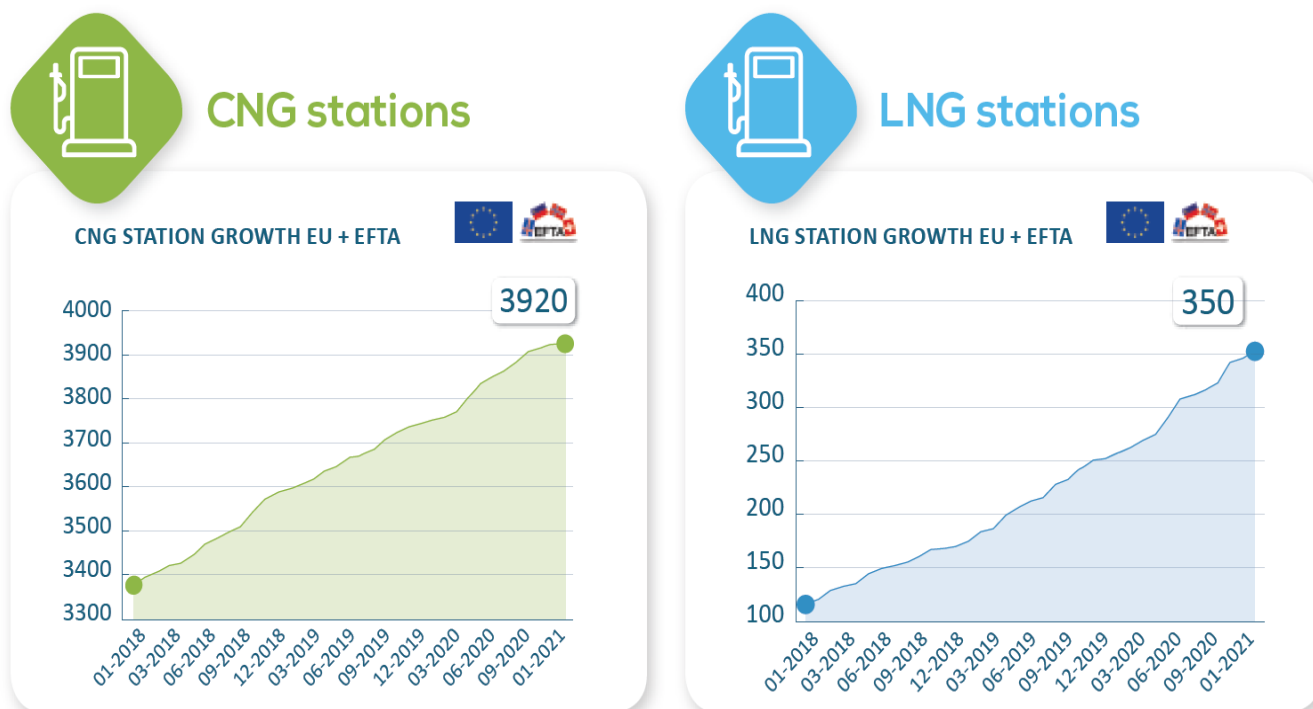
Figure 2. Growth of refueling infrastructure [8]

The number of public hydrogen stations has quadrupled in the last five years.
Below is the number of hydrogen fuel stations at the end of 2019:
- 432 worldwide
- 330 open to the public (worldwide)
- 226 additional filling stations are being prepared in dedicated locations (worldwide)
- 177 in Europe
- 87 in Germany

4. VEHICLE FUEL SYSTEMS

There are three types of vehicles powered by natural gas (NGV):
- Dedicated: Vehicles designed to run on natural gas only;
- Bi-fuel: These types of vehicles have two separate fuel systems. They allow operation on either natural gas or petrol (Figure 3);
- Dual fuel: In the case of these heavy-duty vehicles, a pilot injection of diesel fuel is used to ignite the natural gas.
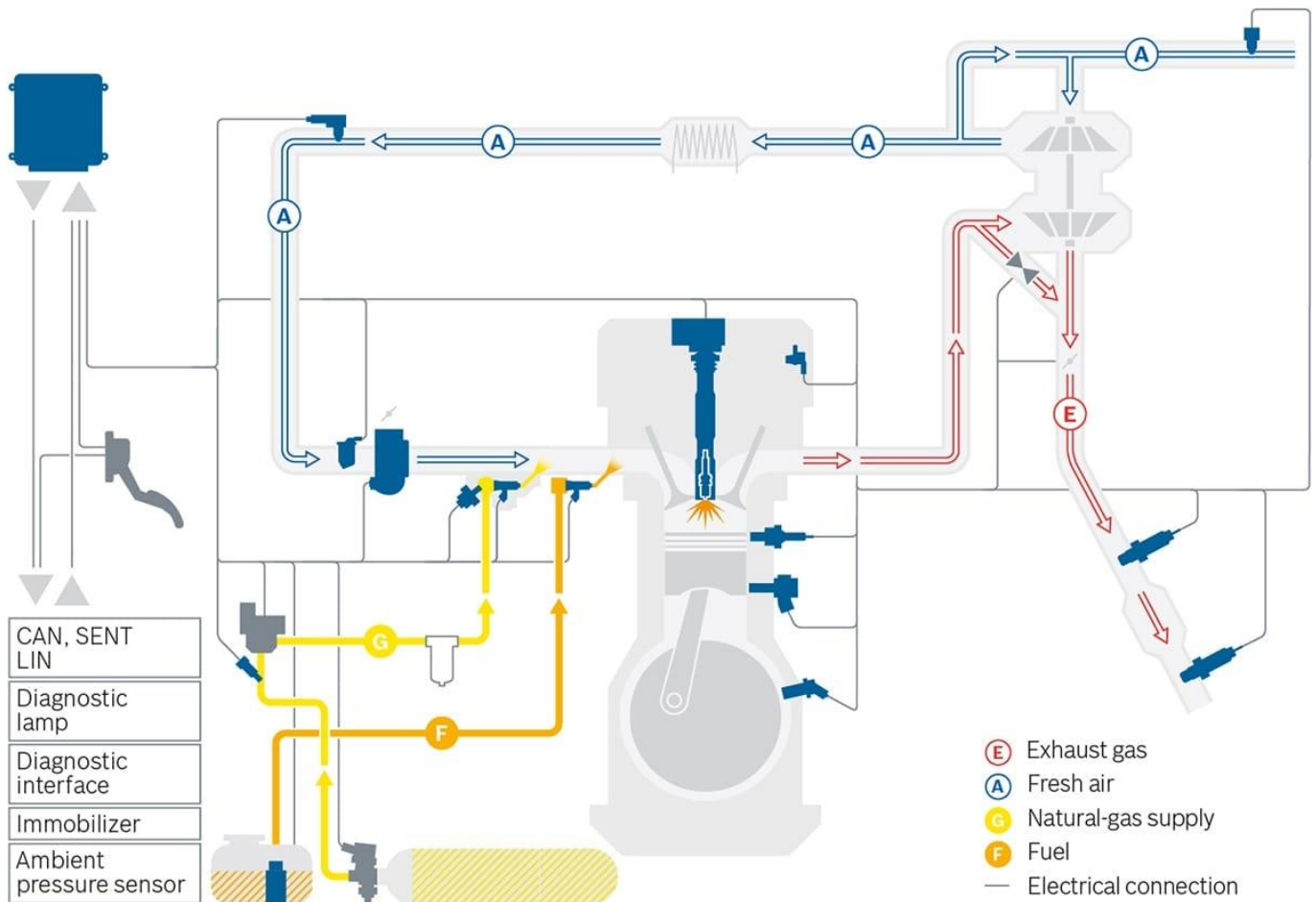
Figure 3. Gasoline – GNC bi-fuel supply system [9]

Usually, light vehicles have a bi-fuel fuel system and heavy vehicles use a dual fuel system.
To increase the autonomy of the vehicles, LNG is used instead of CNG.
LNG is a liquid fuel with a higher energy density than CNG which is gaseous.
CNG vehicles have a lower range than those powered by gasoline or diesel fuel due to the same cause of lower energy density in the case of CNG.

4.1 Natural Gas Vehicles
Natural gas vehicles work similarly to vehicles with spark-ignition engines.
The figure 4 below shows the installation for the supply of compressed natural gas mounted on a vehicle.
The installation consists of a natural gas tank under high pressure, a pressure regulator and injection system for indirect or direct injection.

4.2 Bi-fuel Natural Gas Vehicles
Figure 5 shows the fuel supply installation for a bi-fuel vehicle. In this case, the same engine can be powered by either gasoline or CNG, by pressing a button by the driver.
The system consists of 2 separate systems for each fuel: tank, injection system and fuel pipes.

4.3 Natural Gas Trucks
Natural gas heavy-duty vehicles work similarly to vehicles with spark-ignition engines, but they can also work on compression ignition engines.
The figure 6 below shows the installation for the supply of compressed natural gas mounted on a vehicle.
The installation consists of a natural gas tank under high pressure, usually mounted behind the driver's cab, a pressure regulator and injection system for indirect or direct injection.
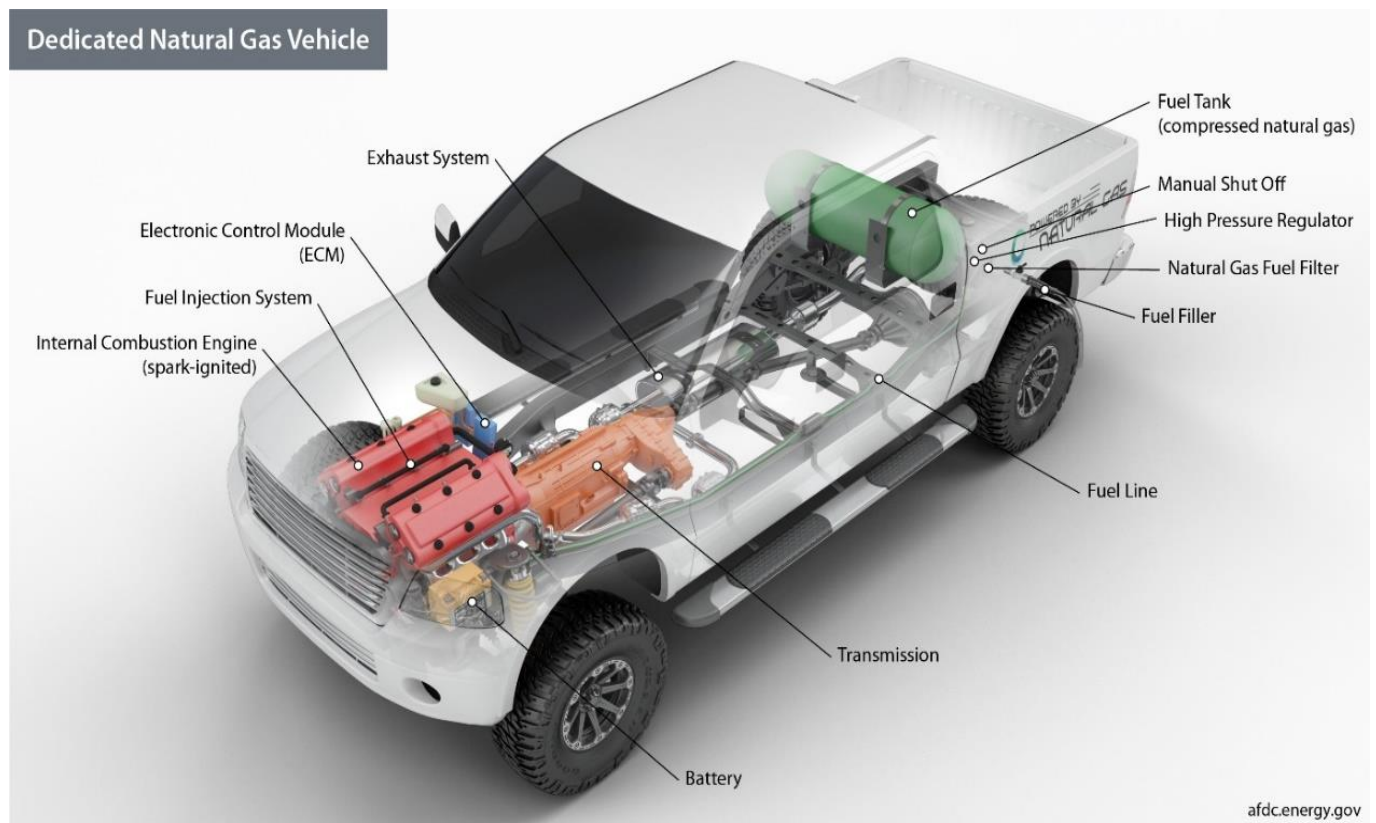
Figure 4. Natural Gas Vehicle [10]
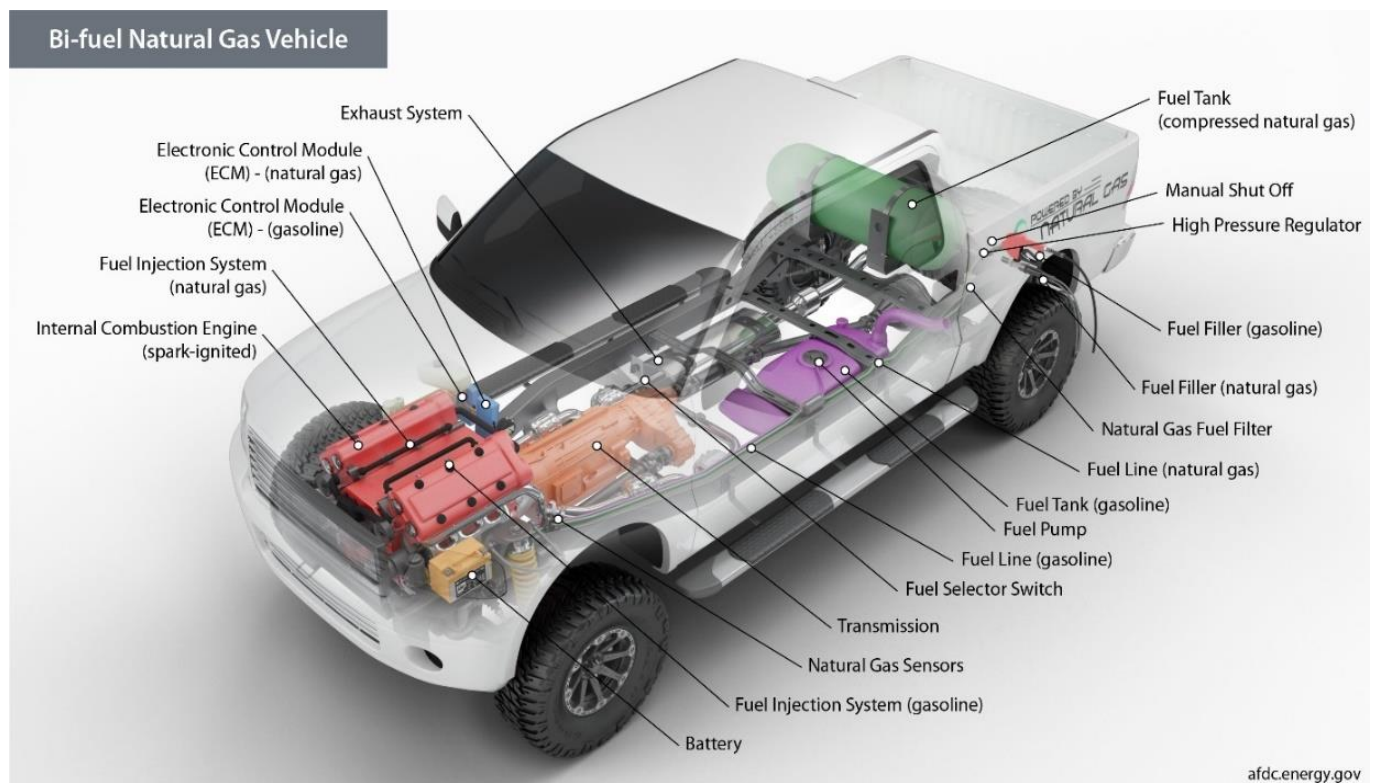
Figure 5. Bi-fuel Natural Gas Vehicle [10]
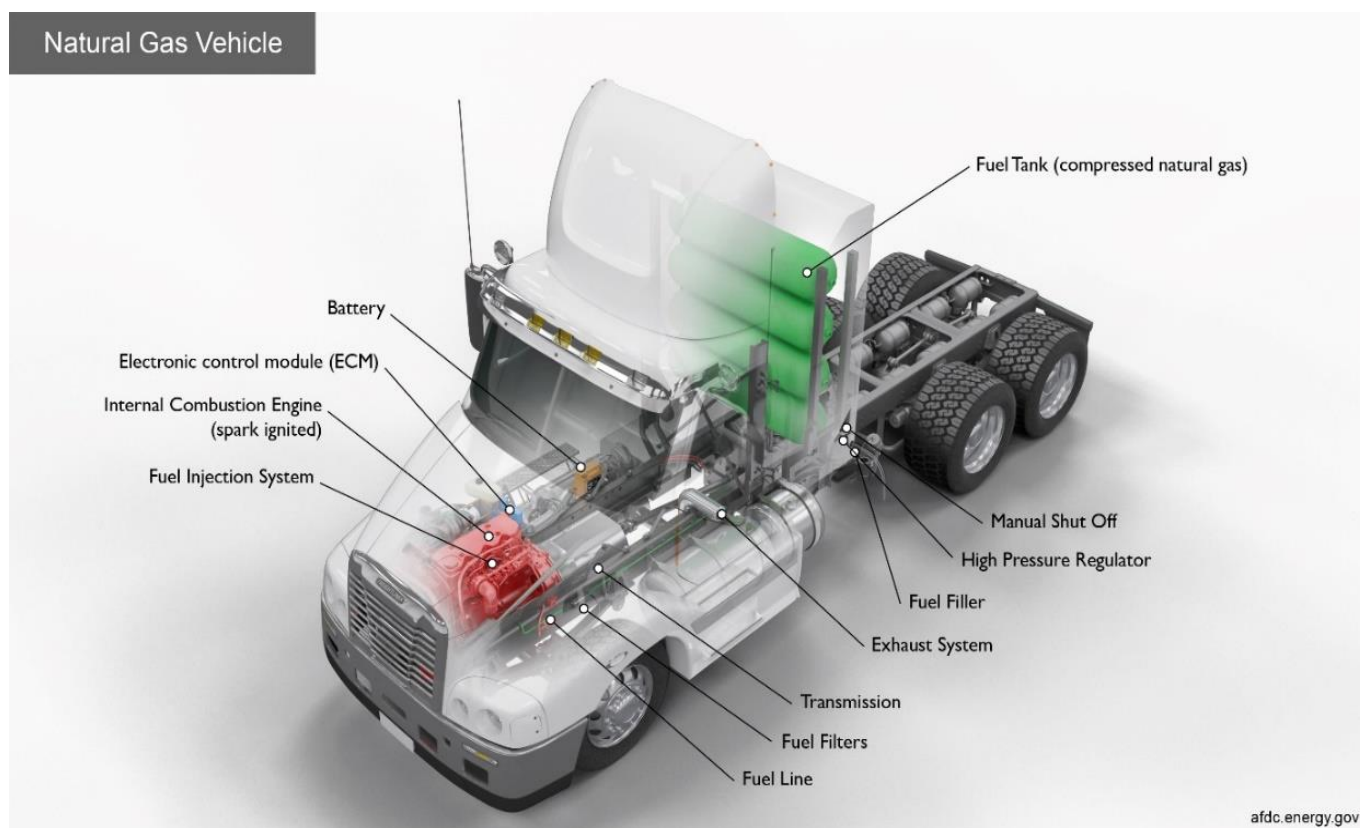
Figure 6. Natural Gas Trucks [10]

5 LEGISLATIONS

5.1 Emission standards

The World Health Organization (WHO) sets air quality standards that are applied in different parts of the world. Air quality primarily affects people's health, which is why we want the lowest possible level of pollutant emissions. Crowded cities are the main concern, especially for emissions particles, NOx and Ozone. Vehicles are contributing mainly to particle and NOx emissions.

Light-duty vehicles emit mainly the following emissions: hydrocarbons (HC), particulates (PM and PN), carbon monoxide (CO), nitrogen oxides (NOx), ammonia (NH3) and specific hydrocarbon components.

Three major test categories are used in the world; the US and some countries in South and Central America use the US testing procedure called FTP; in Europe and in countries that use European legislation, the WLTP procedure and the new Real Driving Emission (RDE) tests have been used since 2017 and in China, elements from both the US and Europe are used (Figure 7).

Whether it is a small class or luxury class car, it must meet the same maximum limits [mg/kg] of the regulations when marketed.

In the figure 8 below it can be seen that from 2023 the regulations in China will be stricter than in Europe. The evolution of emission standards in Europe and the US is shown in Figure 9.

It should be noted that US standards do not consider the type of fuel, gasoline, or diesel, compared to European standards that impose different limits type.

5.2 Corporate Average Fuel Economy regulation (CAFE)

Regulation (EC) 443/2009 sets mandatory emission reduction targets for new vehicles.

The first target has been fully implemented since 2015 and a new target has been gradually introduced in 2020 and will be fully implemented from 2021 [12]. From 2021, gradually introduced in 2020, the average EU-wide emissions target for new cars is 95 g CO_2 / km.

If the average CO_2 emissions of a manufacturer's fleet exceed 95g / km in a year, then the manufacturer must pay 95 euros for each gram of CO_2 exceeded, for each vehicle sold in that year.
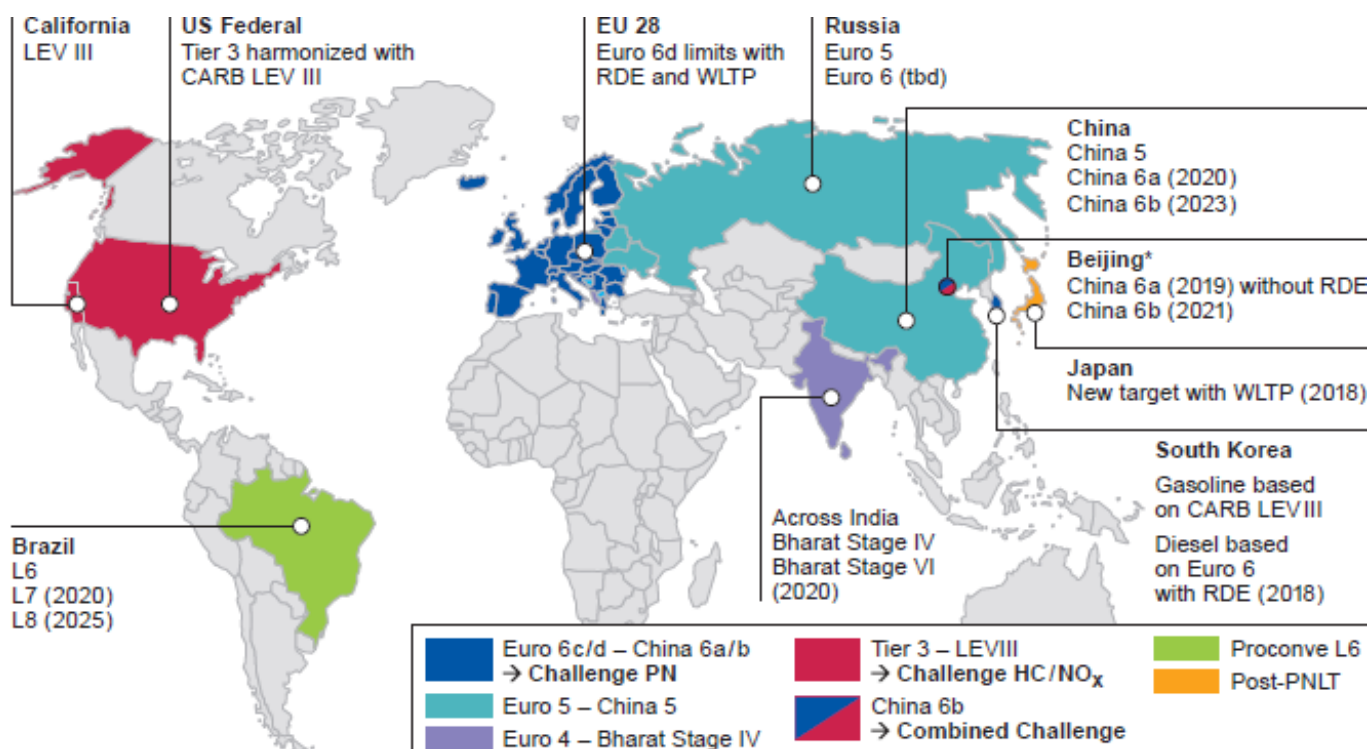
Figure 7. Emission Legislation Worldwide [11]
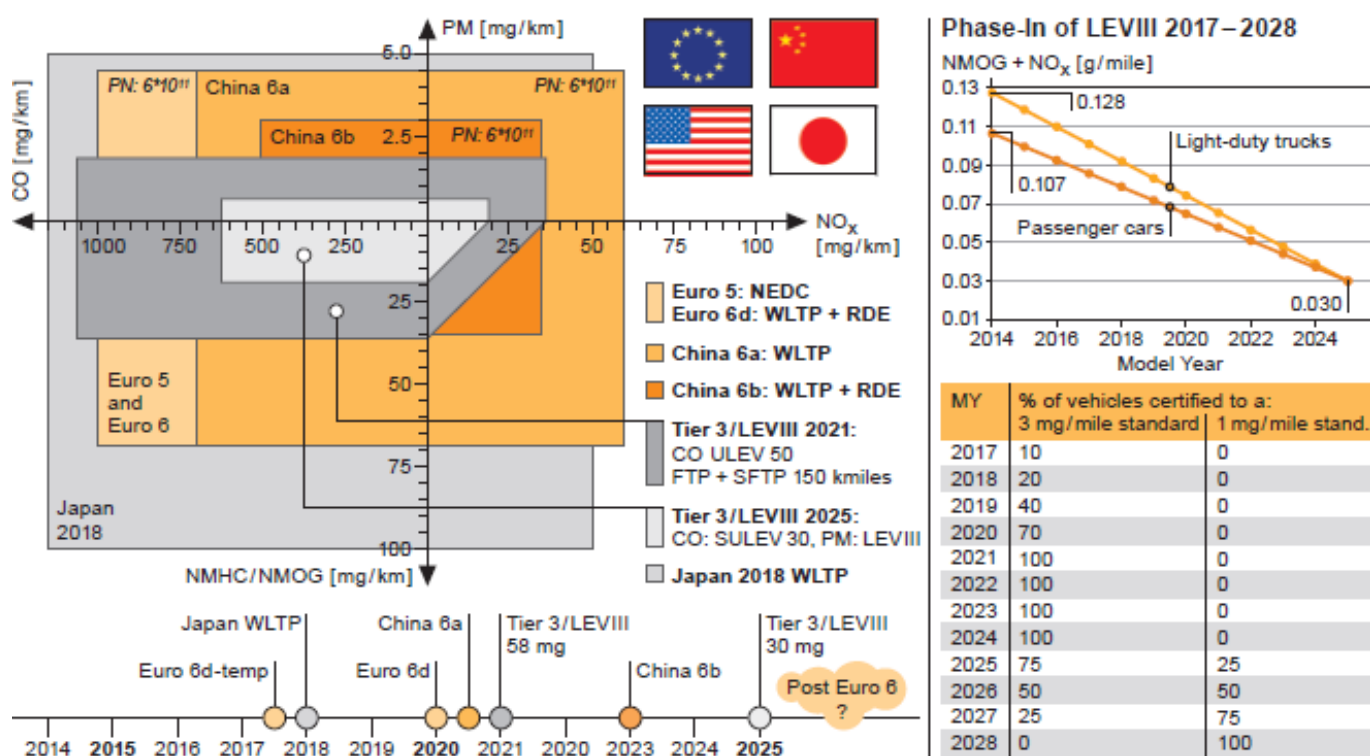
Figure 8. Implementation Date of Emission Limits [11]
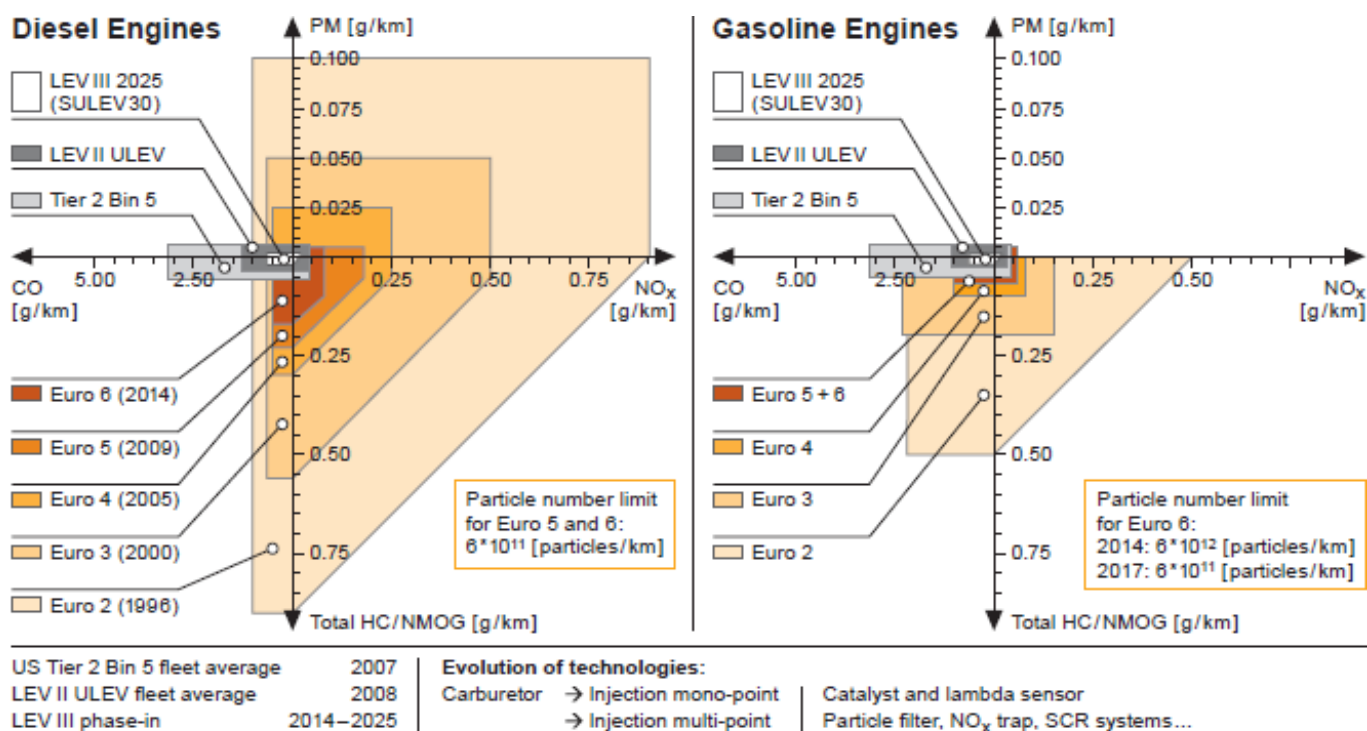
Figure 9. Emission Limits Evolution in Europe and US [11]

6. RESEARCH RESULTS OBTAINED WITH CNG

6.1 Emissions of gaseous fuels

Various tests were performed to highlight the differences between petrol and LPG (for vehicle A) on the one hand and petrol and CNG (for vehicle B) on the other hand.

The results are presented over 3 test cycles: UDC, EUDC and NEDC.

Figure 10 shows the total hydrocarbon emissions (THC), Figure 11 shows the CH4 emissions and Figure 12 shows the methane-free hydrocarbon (NMHC) emissions.

The only differences were observed in the case of vehicle B powered by CNG; THC emissions are 25% higher than gasoline (figure 10) due to values about 7 times higher for CH4 emissions (figure 11) in the UDC cycle.

These very high values for CH_4 emissions are because methane is a compound that is difficult to oxidize in the catalyst. CH4 emissions are not currently regulated directly in Europe but are regulated in the USA because methane is also a greenhouse gas (CH_4 absorbs 21 times more infrared radiation than CO_2) [3]. In Europe, THC is considered, which also includes CH4 emissions.

Methane-free hydrocarbon (NMHC) emissions are about 30% lower than the Euro 6 emission limit (figure 12).

A significant difference for NMHC emissions occurs with the use of CNG (approximately 45% lower than gasoline) due to the low presence of hydrocarbons with more than 2 carbon atoms.

Figure 13 shows the CO_2 emissions. There are decreases of up to 25% for CNG and 10% for LPG.

These decreases are due to the higher ratio of hydrogen and carbon atoms in the molecule of methane and LPG compared to gasoline.

6.2 Emissions and performance using HCNG at lean mixtures

The main drawbacks of natural gas are related to the difficulty of ignition, low flame rate and burning of lean mixtures.

When using CNG, engine efficiency decreases at low loads and we have higher HC and CO emissions, which can be solved using a dedicated catalyst.

To solve some of these inconveniences, adding a small amount of hydrogen can be a solution.

To see the effect of hydrogen addition on the emissions and performance of the HCNG-powered engine, several researchers performed various experiments. One of them is Ali Keshavarz [14] who used a four-stroke, 4.2 L, naturally aspirated natural gas with the results shows to Figure 14: the CO emission depending on the speed for 2 loads (50% and 100% throttle opening).

The lower value in the case of 50% is due to lower pressure and temperature in the engine cylinder [14].
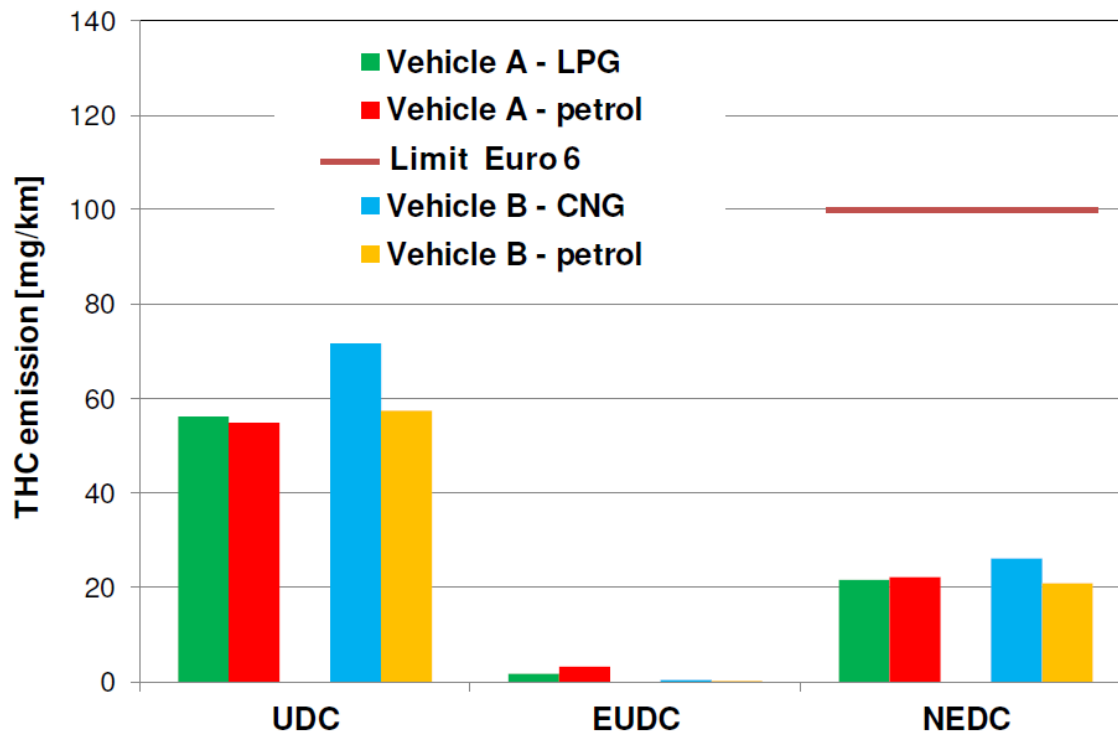
Figure 10. Measured THC emissions [13]
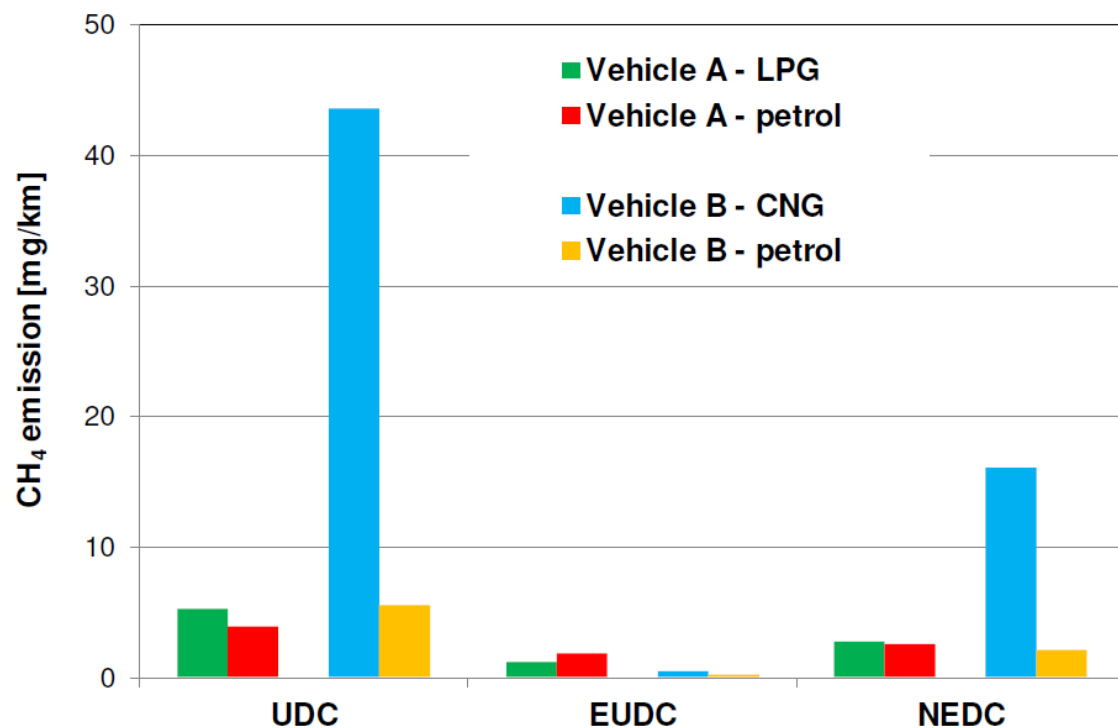
Figure 11. Measured CH4 emissions [13]
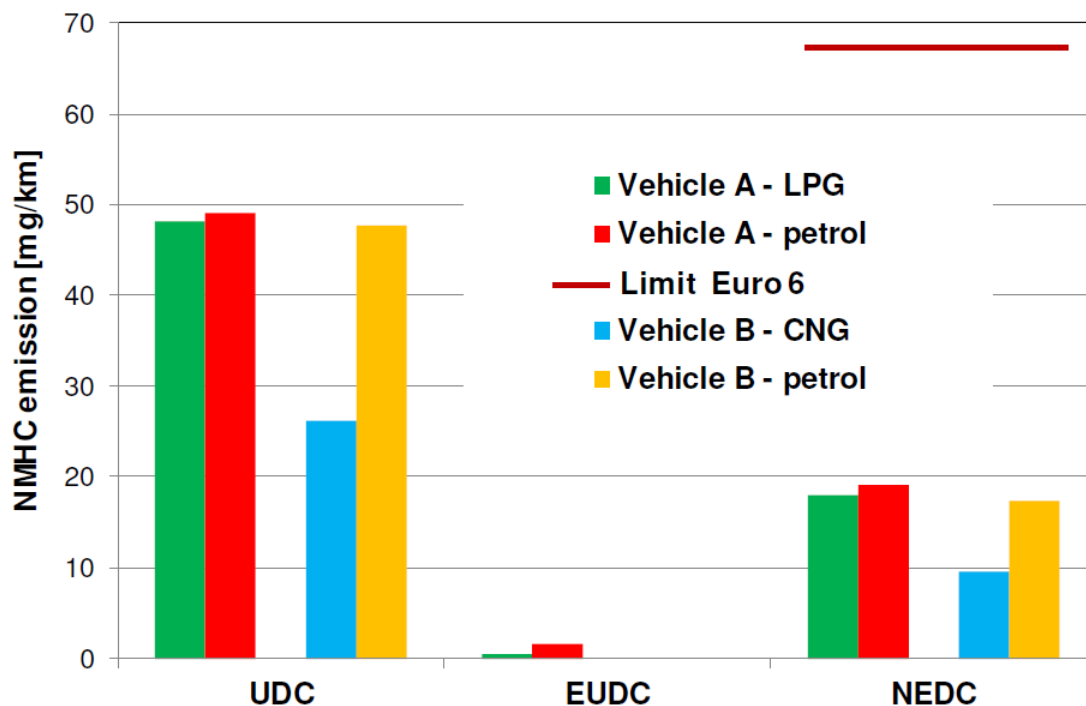
Figure 12. Measured NMHC emissions [13]
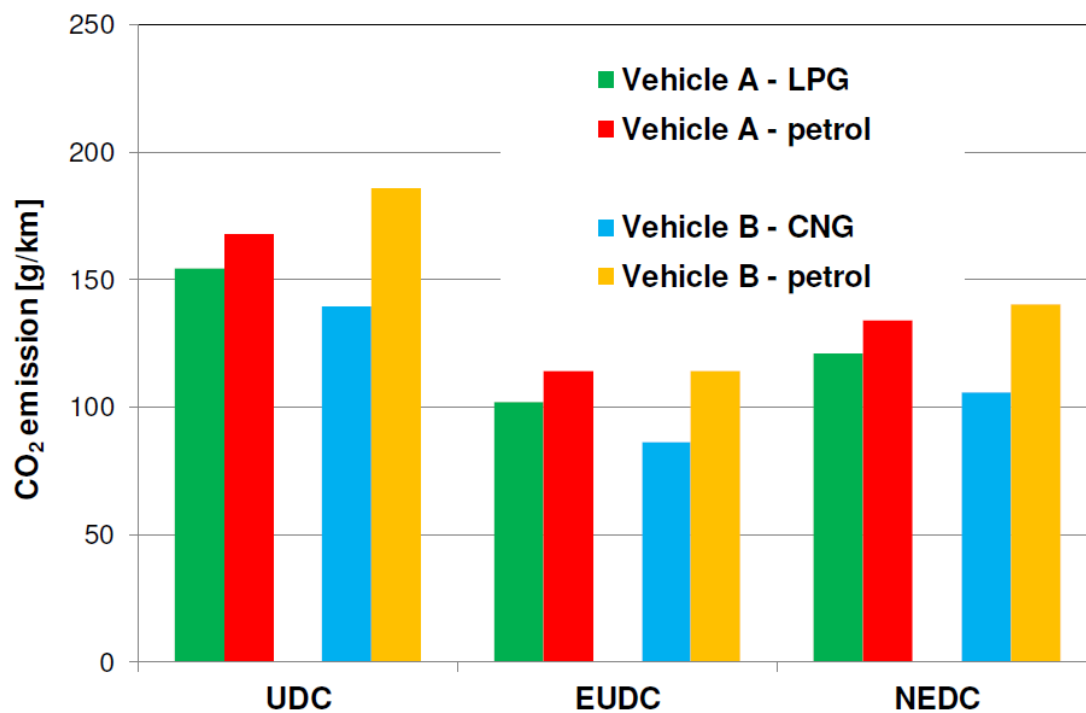
Figure 13. Measured CO_2 emissions [13]

Figure 15 shows the NOx emission depending on the speed for 2 loads (50% and 100% throttle opening). The higher NOx value is measured at maximum load (mainly at 1800 rpm).
Figure 16 shows the brake-specific fuel consumption (BSFC) depending on the engine speed for 2 loads (50% and 100% throttle opening).
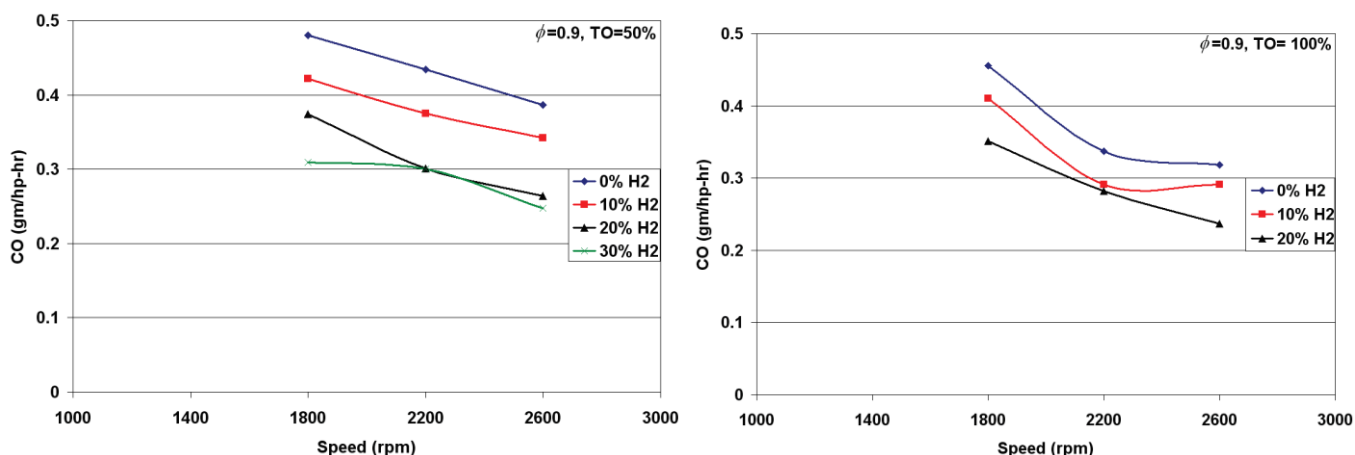
Figure 14. CO emissions for 0.9 fuel-air equivalence ratios [14]
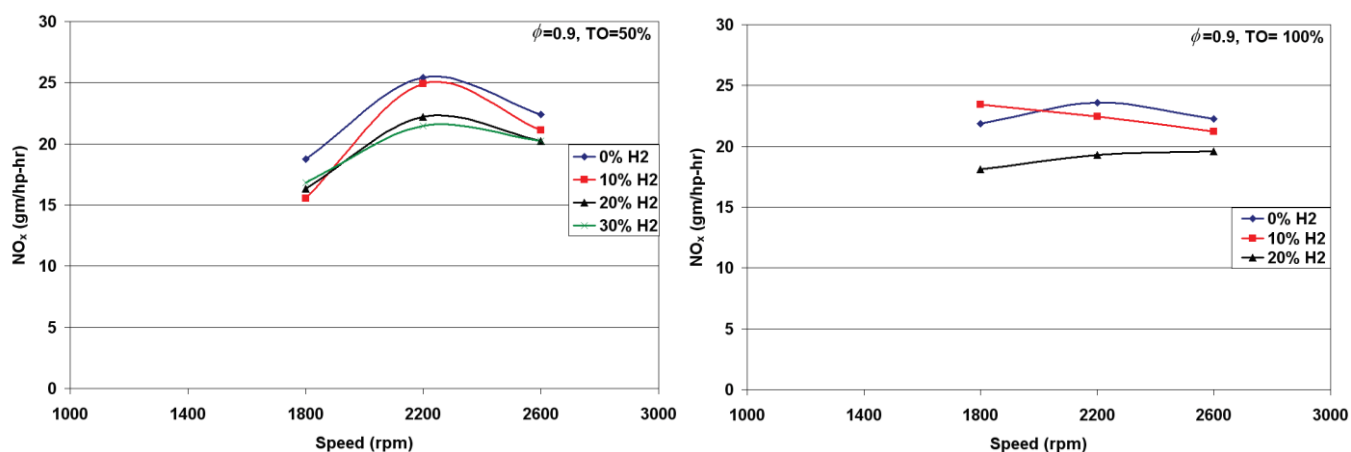
Figure 15: NOx emissions for 0.9 fuel-air equivalence ratios [14]
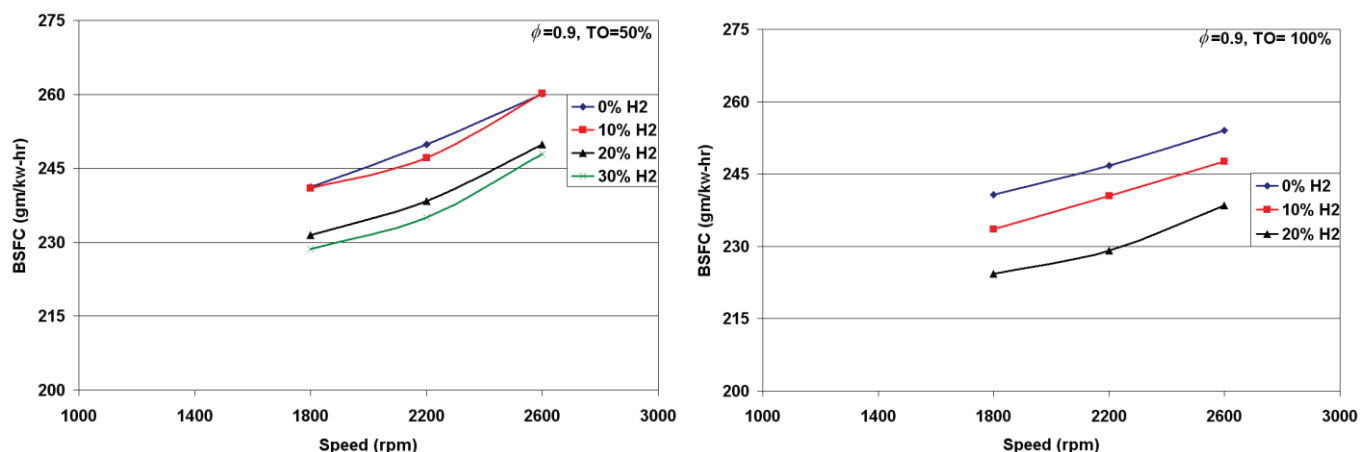
Figure 16. BSFC for 0.9 fuel-air equivalence ratios [14]

6.3 HCNG in Laser and Spark Ignition modes
Another study that reflects the effects on performance and emissions by adding hydrogen to spark-ignition engines powered by compressed natural gas with a laser ignition system is that of R. K. Prasad et al. [15]. In this study an indirect injection spark ignition engine was equipped with two ignition systems: spark ignition (SI) and laser ignition (LI) at 1500 rpm and different brake mean effective pressures (BMEP) and air-fuel ratios (λ).
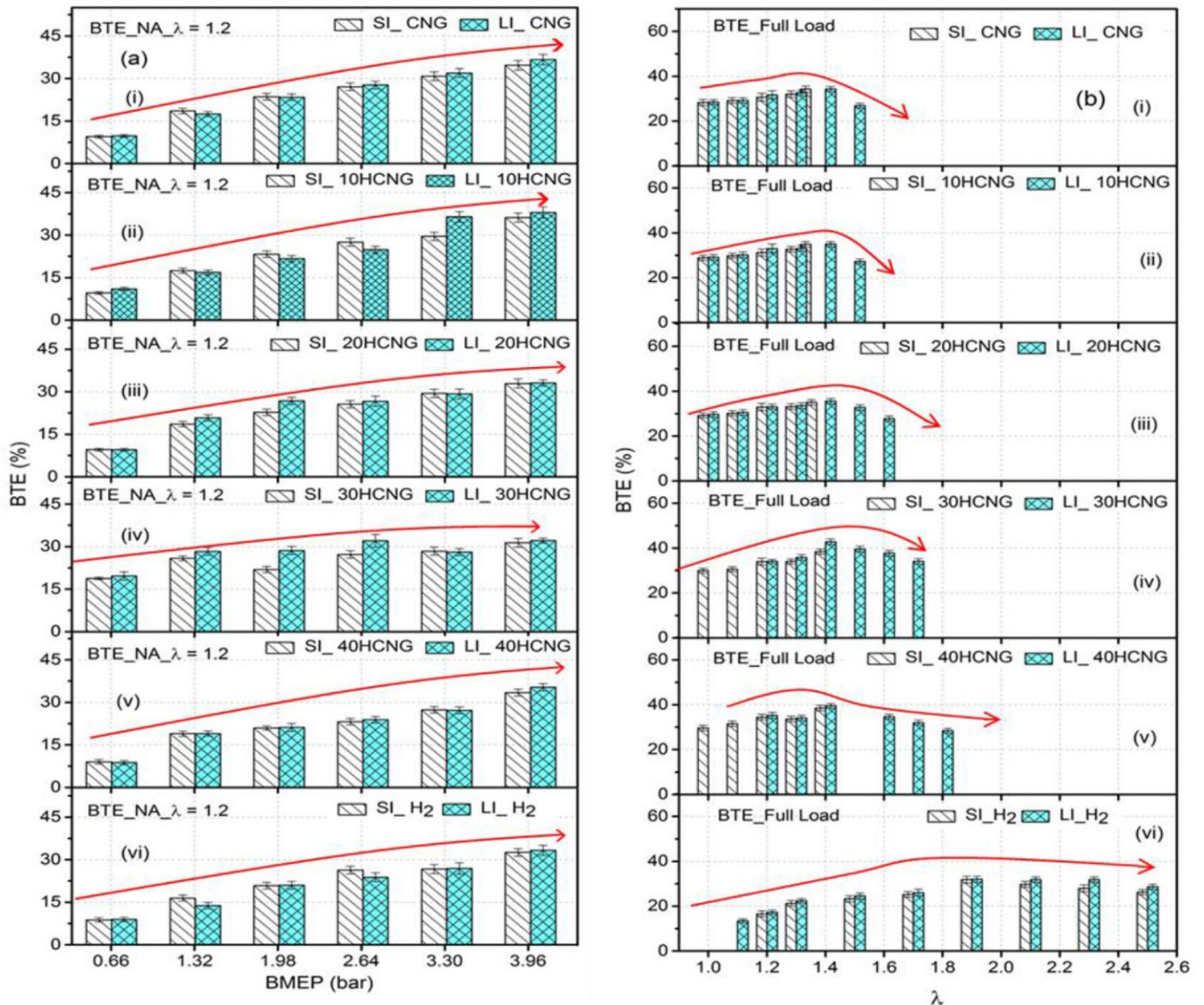
Figure 17 (a, b) BTE variation depending on the type of fuel and the ignition system [15]

The following figure 17 (a and b) shows a comparison of LI and SI ignition modes over the results concerning the variation of the brake thermal efficiency as a function of the BMEP and lambda, and the comparative variation of the brake thermal efficiency according to BMEP and lambda for HCNG mixtures with laser and spark ignition systems.

It can be observed that the efficiency increased once the brake mean effective pressure was increased for all HCNG mixtures (Figure (17a)). Figure (17b) shows the variations of efficiency with lambda at maximum load.

It was observed that with the increase of lambda, in the first phase the efficiency increased and then decreased for all HCNG mixtures.

Hydrogen enrichment has extended the combustion limit fuels HCNG. (Burning limits for CNG and 10HCNG were λ = 1.5; for 20HCNG it was λ = 1.6; for 30HCNG it was λ = 1.7; for 40HCNG it was λ = 1.8 and for H2 it was λ = 2.5).

The next figure 18 shows Brake Specific Nitrogen Oxides (BSNOx) emissions depending on BMEP (figure 18 a) and λ (figure 18 b) using laser ignition and spark ignition modes.

BSNOx emissions increased with increasing BMEP for all test fuels, regardless of ignition mode. NOx formation during combustion occurs mainly due to atmospheric N2 oxidation under high-temperature conditions (> 2000 K) [16].

There was a higher BSNOx emission for both ignition systems, which increased with load (BMEP) due to temperatures above 2000 K which led to the oxidation of nitrogen from the air [16].

A higher value of BSNOx was obtained in the case of CNG laser ignition but also in the presence of hydrogen due to high-temperature combustion peaks due to an earlier start of combustion.

The BSNOx emissions rise from 6 (for CNG) to 12 g/kWh (for 40HCNG) for a load of 3.96 bar [15].

In figure 18 b BSNOx is decreasing for both ignition systems as the air-fuel ratio increase.

This trend was reversed as the temperature decreased due to the excess air that cooled the mixture.

The maximum temperature in the cylinder was lower with the laser ignition system that leads to a decrease in BSNOx emissions.

Figure 18 (a, b) BSNOx variation depending on the type of fuel and the ignition system [15]

7. CONCLUSION

- Faster and higher quality combustion was observed in natural gas engines by mixing with a fast-burning fuel such as hydrogen.
- Nitrogen oxide emissions normally increase with increasing hydrogen due to higher engine cylinder temperatures, but a method of reducing them such as a catalytic converter, NOx Trap, or an EGR system can be used.
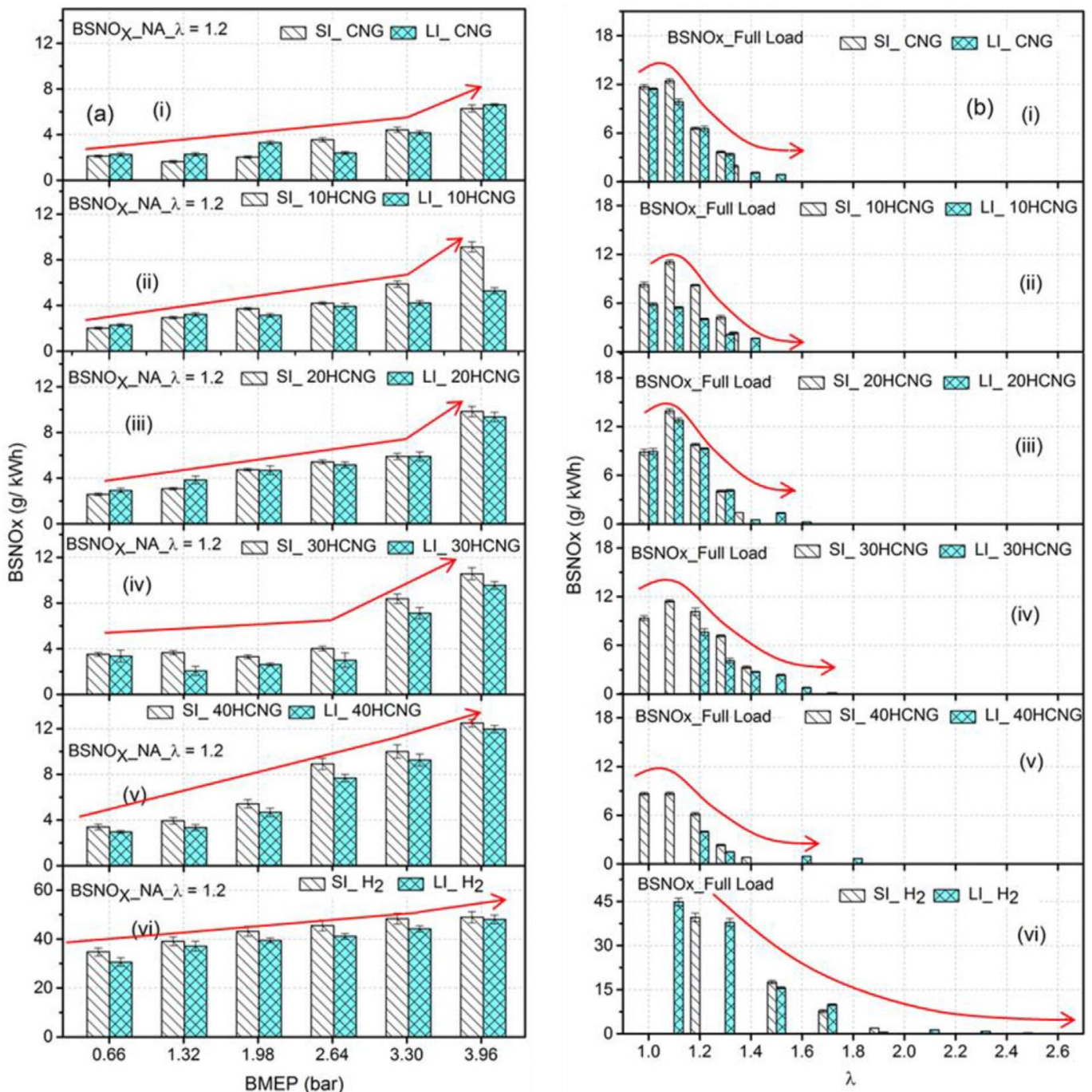- Emissions of hydrocarbons, carbon dioxide and carbon monoxide decrease with the increasing percentage of hydrogen.
- Hydrogen enrichment extends the combustion limit of HGNC mixtures.
- To be able to obtain significantly improved performance characteristics, the compression ratio of the engine can be increased when using CNG and H2 due to the higher-octane number compared to petrol.
- The addition of H2 (up to 20-30% volume) to natural gas can be an effective short-term solution to the problem of greenhouse gases and in addition, no engine modifications are needed with current technology.

REFERENCES

[1] Cho H.M., He B.Q., *Spark ignition natural gas engines – a review*, Energy Convers Manage 2007;48(2):608–18

[2] Fuwu Yan, Lei Xu, Yu Wang, *Application of hydrogen enriched natural gas in spark ignition IC engines: from fundamental fuel properties to engine performances and emissions.* Renewable-and-sustainable-energy-reviews

[3] Seinfeld J H and Pandis S N, *Atmospheric Chemistry and Physics: From Air Pollution to Global Climate Change* Wiley Interscience New York, 1998

[4] Adeeb Z., *Glycerol delignification of poplar wood chips in aqueous medium*, Energy Educ Sci Technol 2004;13:81–8

[5] Tunestal P., Christensen M., Einewall P., Andersson T., Johansson B., Jonsson O., *Hydrogen addition for improved lean burn capability of slow and fast burning natural gas combustion chambers,* SAE paper 2002-02-2686; 2002

[6] Thipse S.S., et al, *Development of a CNG injection engine compliant to Euro-IV norms and development strategy for HCNG operation*, SAE Paper 2007-26-029

[7] Patil K.R., Khanwalkar P.M., Thipse S.S., Kavathekar K.P., Rairikar S.D., *Development of HCNG Blended Fuel Engine with Control of NOx Emissions,* International Journal of Computer Information Systems, and Industrial Management Applications (IJCISIM),
ISSN: 2150-7988, 2010;2:087-095

[8] *The Natural & biogas Vehicle Association*; NGVA Europe, ngva.eu

[9] *System technology for passenger cars and light commercial vehicles powered by CNG* – Bosch mobility solutions

[10] U.S. Department of energy, afdc.energy.gov

[11] Worldwide Emission Standards and Related Regulations - Passenger Cars / Light and Medium Duty Vehicles May 2019; continental-automotive

[12] Official Journal of the European Union - Regulation (Ec) No 443/2009 of the European Parliament and of the Council of 23 April 2009 setting emission performance standards for new passenger cars as part of the Community's integrated approach to reduce CO2 emissions from light-duty vehicles

[13] P Bielaczyc, A Szczotka and J Woodburn. *A comparison of exhaust emissions from vehicles fuelled with petrol, LPG and CNG.* Automotive Research & Development Institute Ltd, BOSMAL, ul. Sarni Stok 93, 43-300 Bielsko-Biala, Poland

[14] Ali Keshavarz, *Experimental Study of Hydrogen Addition Impact on Emissions and Performance of a Natural Gas Fueled Engine.* The Journal of Engine Research / Vol. 14 / 2009

[15] Rajesh Kumar Prasad, Avinash Kumar Agarwal, *Development and comparative experimental investigations of laser plasma and spark plasma ignited hydrogen enriched compressed natural gas fueled engine;* Energy, Available online 13 November 2020, 119282
https://doi.org/10.1016/j.energy.2020.119282

[16] Heywood JB. *Internal combustion engine fundamentals*. New York: Mc Graw Hill; 1988

OPTIMIZING THE THERMAL MANAGEMENT OF INTERNAL COMBUSTION ENGINES BY IMPLEMENTING SPTI

Corneliu BIRTOK-BANEASA[*], Adina BUDIUL-BERGHIAN, Diana Monica STOICA,
Amalia Ana DASCAL, Oana GAIANU

Politehnica University of Timisoara, Hunedoara Faculty of Engineering,
Engineering and Management Department, Piaţa Victoriei Nr. 2, 300006 TIMISOARA, Romania

Abstract: *The study refers to the reduction of heat transfer on the intake system, mainly in the case of the aluminum alloy intake manifold. To this end, a series of solutions for reducing heat loss have been adopted, implemented, and tested. These consist in the design and insulation of the intake manifold with a new type of composite material with thermal insulation, whose composition contains natural, organic, and recyclable elements. To establish the thermal insulation properties of the newly developed materials, the topographic and morphological analysis was performed, respectively determined the values of the heat transfer coefficients. The thermal insulation layer called SPTI (Silicone Polyurethane Thermo-Insulating), offers protection to the thermally stressed components (convection, conduction, and radiation) of vehicles, such as intake manifolds, air conditioning systems, various components of the braking system, etc.*

Key-Words: *engine. intake manifold. heat loss. thermal protection. composite material.*

1. INTRODUCTION

The research on the influence of intake air temperature on fuel consumption shows that the highest value of consumption was 380 g / kWh at an air intake temperature higher than 300C, 4% higher than the lowest temperature air intake of 200C at the same engine speed of 1500rpm [1][2].
Variation in air temperature influences NOx and HC emissions as follows: NOx emissions increased at high temperatures for all loads, and HC emissions decreased at low temperatures [3][4][5][6]. It has been shown that maintaining relatively low coolant and intake air temperatures can reduce NOx emissions by up to 30%; with improvements in specific fuel consumption, carbon monoxide (CO) and HC emissions [7]. Global standards on emissions and environmental constraints, together with the rapid advancement of built-in computing power and new generations of sensors have led to the development of low-temperature combustion engines [8]; The purpose of an LTC-combustion at low temperatures engine is to achieve high levels of combustion efficiency without producing harmful emissions such as nitrogen oxides (NOx) and dust particles (PM) in the case of diesel engines. First, the acquisition and processing of real-time data of the processes in the engine cylinders, so that the engine parameters can be adjusted to obtain optimal performance. Second, precise control of the fuel supply is achieved by using multi-pulse injection systems or the combination of indirect injection and direct injection. Thirdly, an important factor is to maintain control over the combustion temperature by recirculating the exhaust from a previous cycle (EGR) [9].

2. EXPERIMENTAL SETUP

2.1 Topographic, morphological analysis and determination of the heat transfer coefficient of the proposed materials

One method of reducing the heat loss of the intake manifold is to implement thermal protections on its outer surface. The main goal is the development of a new thermal insulation composite material, based on polyurethane foam, silicone, and cork in different proportions [10].

---
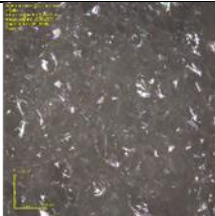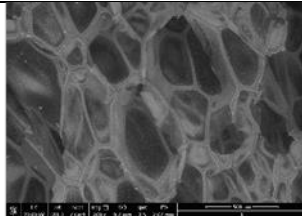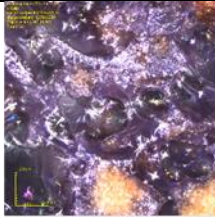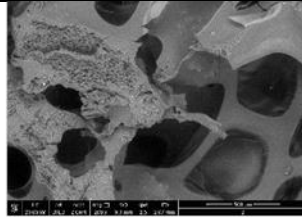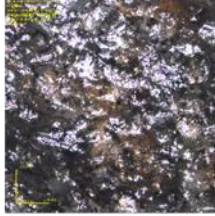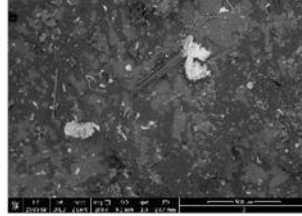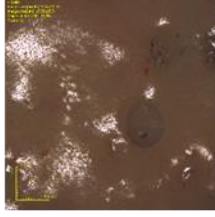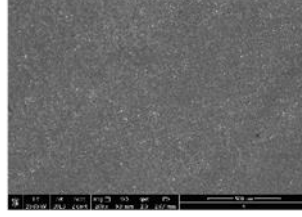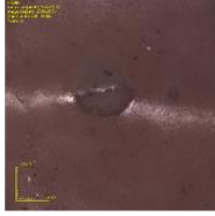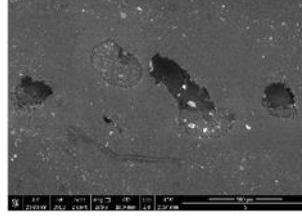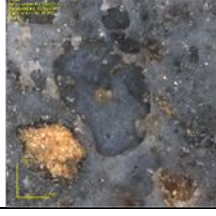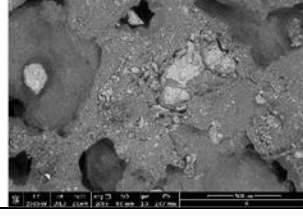
[*] *Corresponding author e-mail:* corneliu.birtok@fih.upt.ro

The topographic and morphological analysis of the samples was performed at the Research Institute for Renewable Energies (ICER) Timisoara using the Olympus OLS 4000 LEXT 3d laser confocal microscope and Quanta FEG 250 microscopes equipped with EDAX analyzer and SDD Apollo detector (SEM and EDX analysis).

Table 1.
Material evidence - topographic and morphological analysis

No.	Sample	Topographic analysis	SEM analysis
1			
2			
3			
4			
5			
6			

From the images presented in table 1, it appears that:
- sample 1 shows a pore depth of (400 - 600) µm and in the EDX analyzed areas the presence of the main elements Cl, Si, C in proportion of over 40% and of the minor components Al, O, N, K, Mg, N and P is observed;
 - sample 2 has a C concentration of more than 65% and the pore depth is between (400 - 800) µm;

- sample 3 shows pores with a diameter of 100 µm and a depth of 800 µm, the main components in the studied areas have a concentration between 30-60%;
- in the case of sample 4, the pore diameter is between (500 - 1800) µm and a depth between (800 - 1200) µm;
- sample 5 shows a porosity with a depth varying between (400 - 500) µm, the component elements having dimensions between (5 - 200) µm;
- in the case of sample 6, the pore diameter is between (400 - 750) µm, with a depth of between (370 - 500) µm.

The standard sample 1, made of polyurethane foam, belongs to the class of thermal insulation materials but due to its relatively low resistance to mechanical stress, it is not recommended to use it in the case of subassemblies subjected to composite stress, such as the intake manifold made of aluminum alloys (subjected to mechanical, thermal, chemical stresses, etc.)

From the analyses presented above, the density and the distribution of pores in the structure of sample 5, are similar to that of the standard sample (polyurethane foam). The silicone concentration (over 50%) of sample 5, leads to the improvement of the elastic properties respectively to the increase of the resistance to compound stresses.

The thermal conductivity for the newly developed materials was determined using the heat flux plate method [10].

2.2 Aluminum alloy intake manifold insulation

To obtain a thermal insulation layer, the material having the composition and structure of sample five, presented in Table 1, with a heat transfer coefficient determined with the value 0,15W / mK [10] was used. The thermal insulation layer was applied on the outer surface of the gallery by brushing (figure 1.a) in several stages, obtaining an average layer thickness of 4 mm.
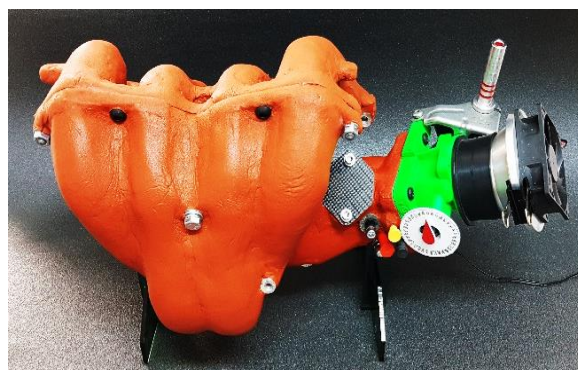
a.   **b.**
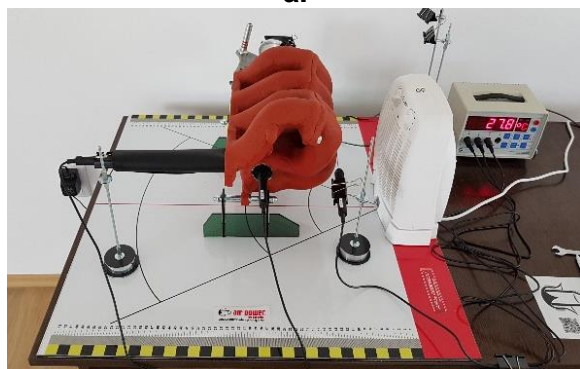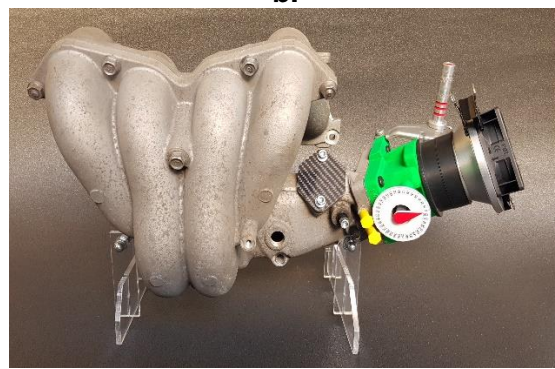
c.   **d.**

Figure 1. Aluminum alloy intake manifold insulated with SPTI:
a – deposition of the insulating layer, b - aluminum alloy gallery protected with SPTI,
c - testing on the RIMS stand, d - aluminum alloy gallery

The gallery protected with the SPTI layer (figure 1.b) was mounted on a stand, own design called RIMS (Resource Intake Manifolds Stand), which allows temperature and pressure measurements at different

characteristic points, for identical or different intake manifolds from a geometric point of view, made of various materials (aluminum alloy, polyamide, composite material, etc.) [10], shown in Figure 1.c.

Previously, on the RIMS stand, the aluminum alloy intake manifold (figure 1.d) of the 1.7 Ford Puma engine was tested, finding relatively high heat losses influenced by the value of the heat transfer coefficient (110W / mK) [10].

3. RESULTS AND DISCUSSIONS

Figure 2 shows the variation of temperatures in the three measuring points (T1, T2, T3) from which the maximum values are found, as follows:

- at the level of the outer surface of the intake manifold 48,10C (T1);
- on the surface of the inner wall 26.70C (T2);
- the intake air at 23,10C (T3).
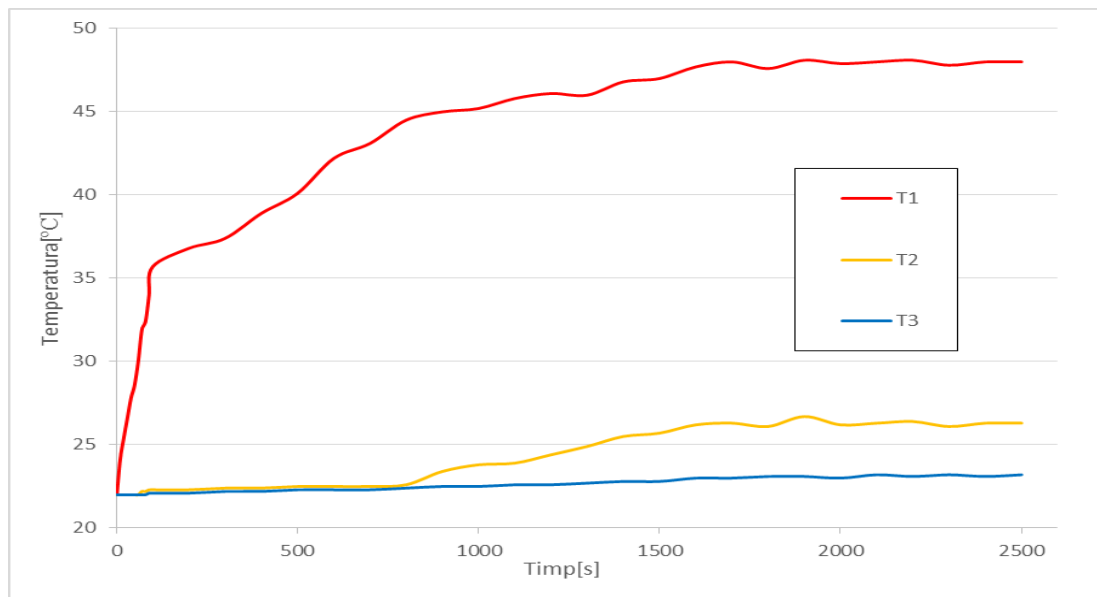
Figure 2. Temperature variation in points T1, T2, T3, in the case of the aluminum alloy gallery protected with SPTI
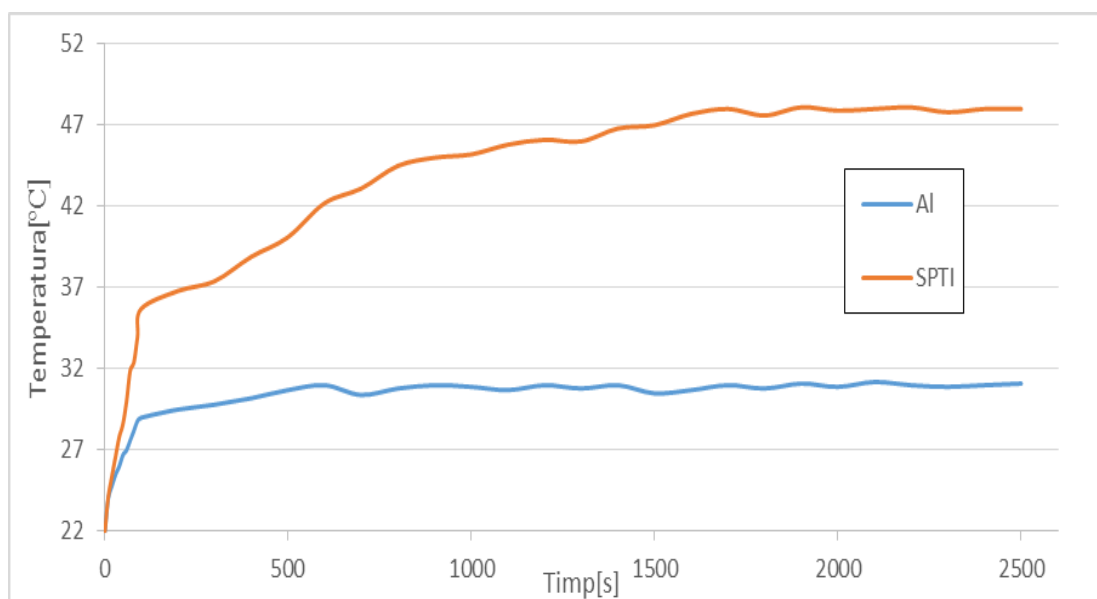
Figure 3. Temperature values at the outer surface of the intake manifolds (T1), aluminum alloy intake manifold / SPTI-protected aluminum alloy intake manifold

The graphs in Figures 3, 4 and 5 show the comparative temperature variations recorded in the case of the intake manifold made of unprotected aluminum alloy and the gallery of aluminum alloy insulated with SPTI.
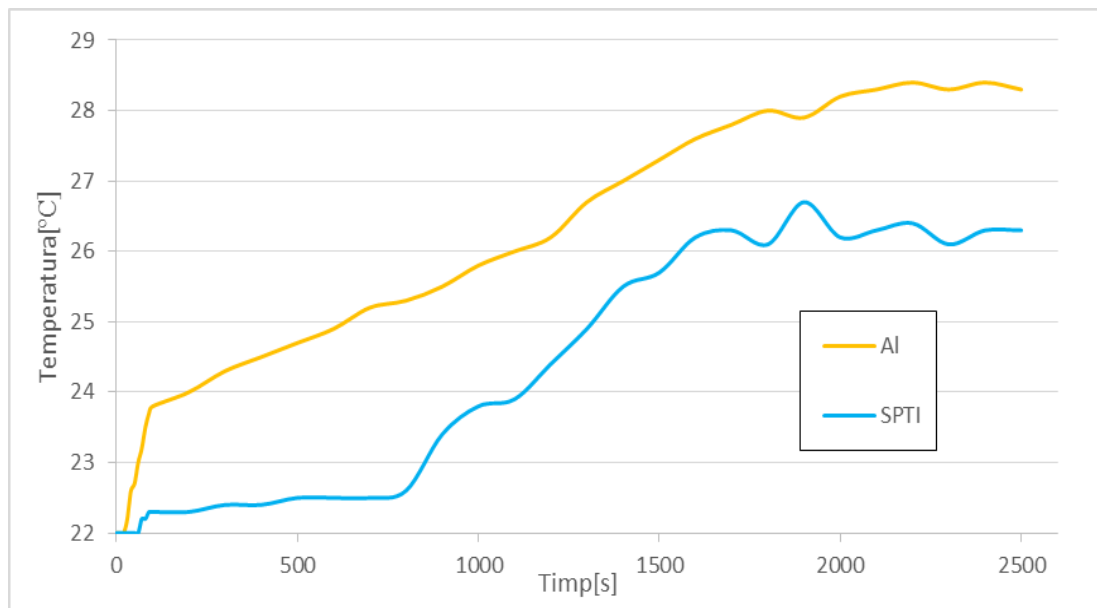
Figure 4. Air temperature on the inner surface of the intake manifold walls (T2)
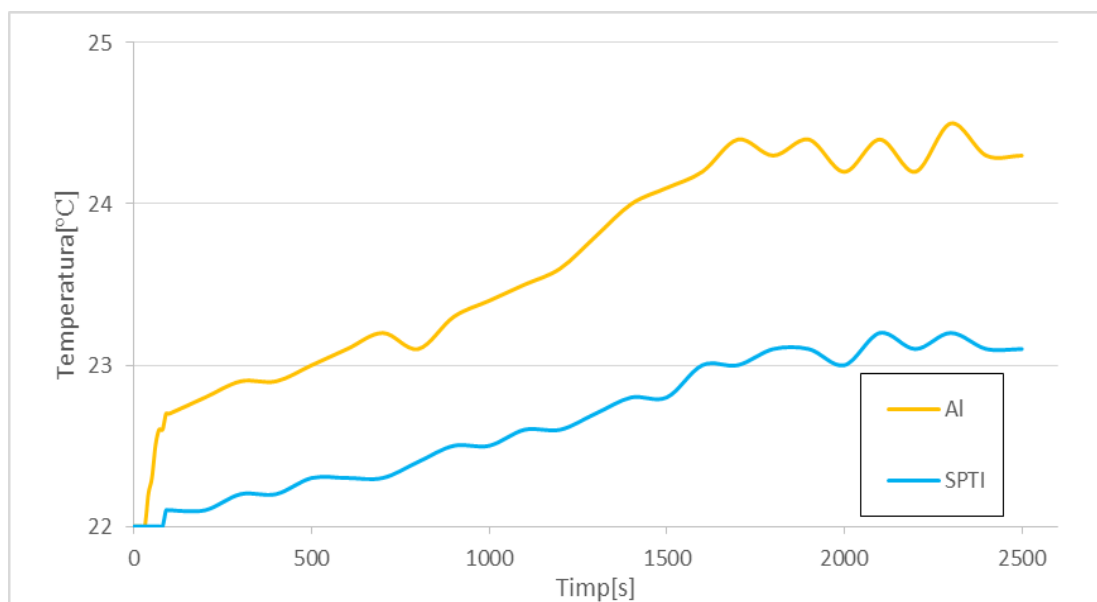
Figure 5. Air temperature at the outlet of the intake manifold (T3), aluminum alloy intake manifold / aluminum alloy intake manifold protected with SPTI

Figure 3 shows that the temperature at the measuring point T1 for the intake manifold protected with SPTI material, shows an increase of 35% compared to the aluminum alloy intake manifold in the unprotected version.

At measuring points T2 and T3 (figures 4. and 5.) the temperatures recorded for the aluminum alloy intake manifold insulated with SPTI show a decrease of 5.96% and 8.33% respectively compared to the aluminum alloy intake manifold in the variant uninsulated

4. CONCLUSION

The main purpose of the experiments performed and presented in this study is to develop new composite insulation materials, natural and organic materials and recyclable materials, designed to reduce heat loss on the intake path.

The determined values of the heat transfer coefficients place the new materials studied in the range of thermal insulation materials and therefore can be used to reduce heat loss in the case of the intake system of internal combustion engines. It is found that the temperature at the measuring point T1 (at the level of the outer surface) for the intake manifold protected with SPTI (silicone polyurethane thermo-insulating) insulating material, increases by 35% compared to the aluminum alloy intake manifold, in the uninsulated version.

The recorded suction air temperature for the aluminum alloy intake manifold insulated with SPTI shows a decrease of 8.33% compared to the aluminum alloy intake manifold in non-insulated version.

REFERENCES

[1] Abdullah, N R; Hazimi, I; Zeno, M; Asiah, A; Hazim, S; *Effects of air intake temperature on the fuel consumption and exhaust emissions of natural aspirated gasoline engine*, Jurnal Teknologi Sciences & Engineering eISSN 2180–3722, 2015;

[2] Birtok Băneasă, C; Raţiu, S; Heputʻ, T; *Influence of intake air temperature on internal combustion engine operation*, IOP Conference Series: Materials Science and Engineering,volume 163/2017;

[3] Gupta, H; *Fundamentals of internal combustion engines*, PHI Private Ltd, India, Delhi, 2013, ISBN 978-81-203-4680-2;

[4] Yoshizaki, K N and Hiroyasu, H; *Approach to Low NOx and Smoke Emission Engines by using Phenomenological Simulation*, SAE Paper 930612, 1993;

[5] Ogawa, K R; Ilizuka, K; and Miyamoto, N; *Cycle-to-cycle Transient Characteristics of Diesel Emissions during Starting*, SAE Paper 1999-01-3495, 1999;

[6] Torregrosa, A; Olmeda, P; Martín, J; and Degraeuwe, B; *Experiments on the Influence of Inlet Charge and Coolant Temperature on Performance and Emissions of a DI Diesel Engine*, Experimental Thermal and Fluid Science, Vol. 30, No. 7, pp 633-641, 2006;

[7] Pang, H; Brace, C; and Akehurst, S; *Potential of a Controllable Engine Cooling System to Reduce NOx Emissions in Diesel Engines*, SAE Technical Paper 2004-01-0054, 2004;

[8]http://www.ni.com/white-paper/13516, *Subsystems Required to Control Low Temperature Combustion Engines*, Publish Date: Apr 20, 2017;

[9] Abdullah, N R; Shahruddin, N S; Mamat, A M I; Kasolang, S; Zulkifli, A; Mamat, R; *Effects of Air Intake Pressure to the Fuel Economy and Exhaust Emissions on a Small SI Engine*, Procedia Engineering, Volume 68, 2013, Pages 278-284;

[10] Birtok Băneasă, C; Rațiu, S; and Heput, T; *Calculation of Thermal Conductivity for New Materials Used in Intake Systems of Internal Combustion Engines*, AIP Conference Proceedings   ICNAAM 2016, 19-25 September, Rhodes, Greece, Mathematical Methods in Economics and Engineering, 1863, Article number 130008, 2017.

EXPERIMENTAL DETERMINATION OF THE FILTRATION CAPACITY FOR CERAMIC FILTER ELEMENTS PROTOTYPES

Robert BUCEVSCHI[*], Ana-Virginia SOCALICI, Adina BUDIUL-BERGHIAN, Corneliu BIRTOK-BĂNEASĂ

Politehnica University of Timisoara, Hunedoara Faculty of Engineering,
Engineering and Management Department, Str. Revoluției, Nr. 5, 331128 HUNEDOARA, România

Abstract: The paper presents the results obtained from the experimental analysis of the filtration efficiency carried out on two filter elements prototypes, developed to filter the air in the passenger compartment of vehicles. The innovation of these concepts is the exclusive use of a porous ceramic mix as a filter medium. The released results also show the influence of the ceramic filter medium granulation on the pressure drop and retention efficiency.

Keywords: Filtration; Porous ceramics; Retention efficiency

1. THEORETICAL MOTIVATION

In order to develop a filter element with a high filtration efficiency for both case of different particles sizes and gaseous pollutants, we take into consideration the analysis of porous ceramic materials behaviors in the filtration processes. These filter elements to be analyzed based on two filter characteristics, the primary stage for the retention of particles and aerosols, and the secondary stage intended to retain the polluting components present in the mixture. This paper presents the method and results of the experimental activities carried out in order to determine the effectiveness of the primary stage [2][5].

Porous ceramic materials can be molecular sieves with pores of uniform size, porosity diameters are similar to the size of small molecules, making it possible to filter or absorb them. As a mixture of molecules migrate through the stationary bed of porous material called sieve, molecular components with the highest molecular weight (which are unable to pass through the molecular pores) leave the first bed by successive smaller molecules. Molecular sieve diameters are measured in ångströms (Å) or nanometers (nm), according to IUPAC (International Union of pure and applied Chemistry), porous materials having pore diameters less than 2 nm (20 Å) may be called micro-porous materials, and the macroporous materials are those having pore diameters greater than 50 nm (500 Å). Pore diameter materials between 50 nm (500 Å) being considered as mesoporous. Of the most common micro-porous materials used in the form of a molecular site we can call: Zeolites, active carbon, Monmonirolite or porous glass [1][4]. To determine the particle retention capacity of the ceramic mixture analyzed in this study, the PAF 113 adsorption test stand was used for the air filters intended for the passenger compartment. The design of the PAF 113 test stand, as well as the test procedure and data acquisition were based on the design standard DIN 71460-1.2 and the standard ISO 11155-1.2.

2. TESTING PROCESS DESCRIPTION

The test stand consists of a conductive and grounded vertical test section, provided with a frame on which the tested filter will be mounted (figure 2), the test chamber being designed to minimize particle losses. The stand also has equipment for air conditioning and supply, flow measurement, pressure loss measurement, aerosol introduction and sampling.

The PAF113 system also has sealing elements so that uncontrolled leaks are less than 100 l / min when the pipe pressure exceeds 500 Pa under ambient temperature conditions (23 ° C). The uniformity of the air flow in the test chamber was measured with a calibrated anemometer, in the center of each of the four areas of equal size and in the center at a distance of no more than 5 cm above the filter holder.

---

[*] *Corresponding author e-mail:* robert.bucevschi@yahoo.ro

The variation of the air flow velocity being less than 10% of the average flow velocity. During the test, the temperature (23 ° C) and the humidity of the test air were maintained at 50%.
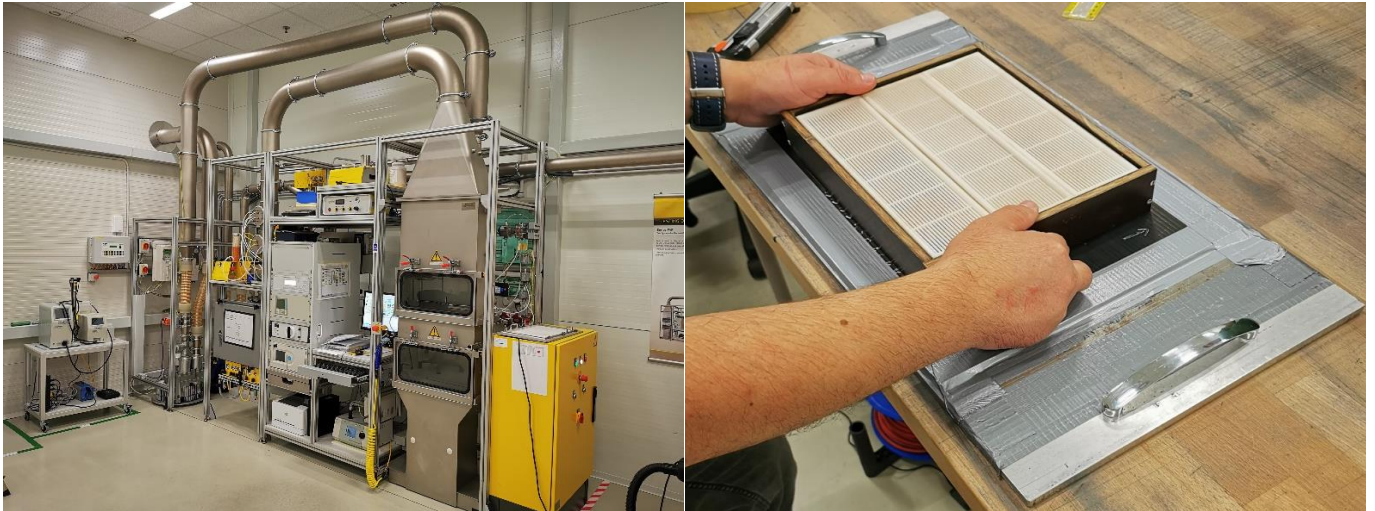
Figure 1. Topas PAF113 test installation   *Figure 2. Attaching the filter to the mounting frame*

The system also has the capability to provide a variable flow rate, specified according to the test method chosen by the user, who can maintain this flow during a test under increasing differential pressure. The maximum flow is up to 680 m³ / h, with filter pressure losses of up to 1,000 Pa.

In the investigation carried out on the porous ceramic filter elements, the flow variation followed the profile described in figure 4, thus for each flow measurement point a 30-second level was generated to stabilize the air flow. The pressure loss (differential pressure) at the tested filter was measured with a differential pressure measuring device connected to the pressure valves in the test line. These valves being in straight sections, have the same cross-sectional area as the section which includes the filter under test and which are not positioned at distances greater than the value of the pipe diameter, upstream and downstream of the test filter. Pressure measuring valves are specific for measuring static pressure [3].

1 - aerosol injector
2 - upstream sampling probe
3 - mounting frame
4 - tested filter element
5 - downstream sampling probe

X - pressure ports
Y - supply nozzle
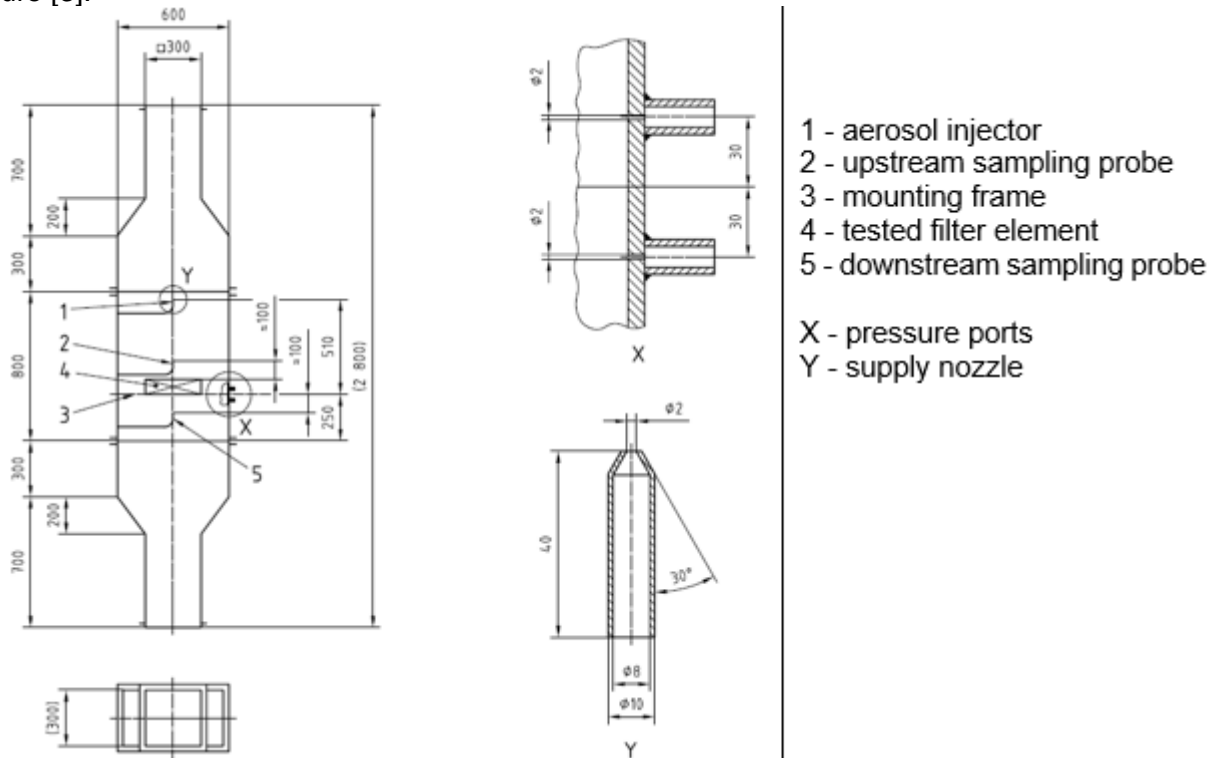
Figure 3. Schematic representation of the test chamber
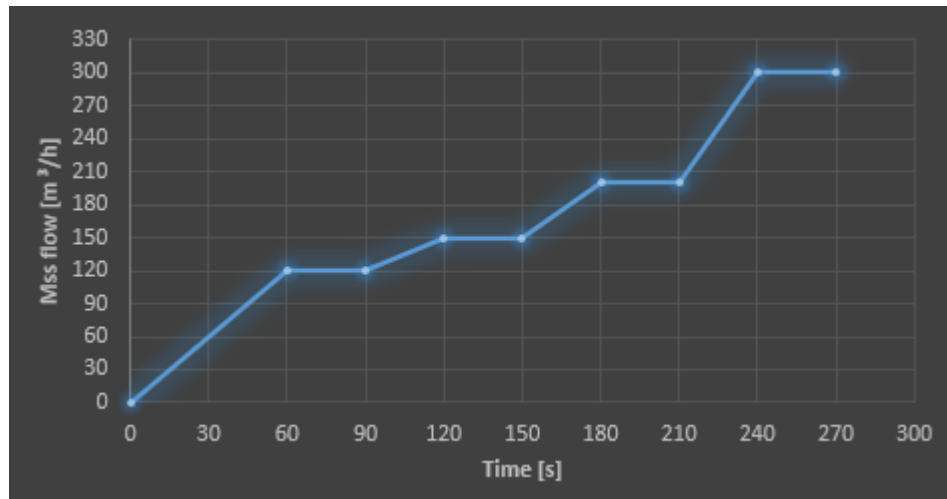
Figure 4. Mass flow rate variation during test procedure

Prior to aerosol mixing, the air was filtered to less than 1% aerosol concentration at all particle sizes, using a HEPA filter. The aerosols were introduced into the duct and subsequently mixed so that a uniform mixture of test aerosols was delivered to the filter under test. The test filter was sealed when mounted on the test frame. The aerosol being taken both upstream and downstream of the filter under test. The sample is then aspirated through the sampling apparatus into a particle counter. The sampling probes are isokinetic (the local flow rate at the pipe level is equal to the flow rate at the well level), the same probe model being used both before and after the filter. The sampling probes were placed on the center line of the test line. Upstream probe at about 100 mm upstream of the test filter and downstream probe 75 mm downstream of the active area of the filter in the center of the pipe and filter. The path of the tubes leading to the particle counter is short to minimize the number of curves to avoid any static accumulation. The materials used in the construction of the routes being earthed electrical conductors, the routes of the upstream and downstream sampling pipes being identical. The aerosol generator used for fractional efficiency measurement tests uses potassium chloride test powder. The aerosol generator used in fractional efficiency tests with capabilities to produce a stable aerosol concentration and size distribution. Thus, ensuring that the particle size distribution of the aerosols contains sufficient particles for statistical evaluation within each size class.

The dust feeder feeds the dust in a continuous and uniform rhythm, with a stable size distribution. An injector is used to disperse the dust into the test system and must not change the particle size distribution in the air. The dust supply system produces an aerosol of a stable concentration (the variation of the maximum allowed concentration over time being 20%).

Figure 5. Potassium chloride used in the testing process

Figure 6. Dust feeder

To minimize the deviations of the results quantified by the particle counter, a particle spectrometer was used which directly measures the aerodynamic size of the particles.

3. THE TESTED FILTER ELEMENT CHARACTERISTICS

The concept of tested filter element is composed of two elements:
- Rigid housing (figure 7).
- The filter element itself in the form of a porous ceramic mixture (figure 8).
The rigid filter housing allows one of the side walls to be detached to replace the worn filter element. This approach aims to reduce the negative impact on the environment by reusing the rigid housing.

Figure 7. Filter rigid housing

In the analysis presented in this article, two types of porous ceramic mixture were tested, with slightly different composition:
The composition of the mixture no. 1: - Soda lime (5-6mm pellets)
          - Activated carbon (5-6mm pellets)
The composition of the mixture no. 2: - Soda lime (5-6mm pellets)
          - Zeolite A5 (0.5-0.6mm pellets)
          - Active carbon (in the form of foam)

Figure 8. Ceramic mix no. 1 (left), and no. 2 (right)

The motivation for using the component materials in the ceramic mixture is the retention properties of the different gaseous components. Sodium lime or soda lime with the following constituent's calcium hydroxide Ca (OH) 2 (70 ... 80%), water H_2O (16 ... 20%), sodium hydroxide NaOH (1 ... 2%) and hydroxide of potassium KOH (> 0 ... 1%) has carbon dioxide retention properties and is commonly used in closed-circuit respirators. Zeolites have an aluminum-silica ratio of ≈2. They are used for drying natural gas, together with desulfurizing and decarbonizing the gas. They can also be used to separate mixtures of oxygen, nitrogen, hydrogen, and hydrocarbons from branched and polycyclic hydrocarbons.

Activated carbon being one of the most widely used porous materials in filter elements, it has the property of retaining particles and aerosols with diameters larger than 0.1 μm, and the pollutant components present in the gas mixture.

4. DISSEMINATION OF THE RESULTS

After the testing process and the acquisition of data using the control unit, data were collected on the pressure drop generated by the filter element, as well as the aerosol retention efficiency over a size range between 0.33-4.77 μm. To determine the pressure, drop generated by the filter element, the pressure drop generated by the rigid housing of the filter was previously measured and will be subtracted from the total value of the pressure drop. Following the post-processing of the data obtained or the graphs of the pressure drop as well as of the retention efficiency/ The graph shows that the introduction of low-granulation components into the mixture led to an average percentage increase in pressure drop by up to 42%. This behavior can be attributed to the increase in the density of the filter element. Also analyzing the retention efficiency, we can see a considerable improvement in the case of prototype no. 2 on the size range 0.44-1.62 μm. During this period there was an average percentage increase in efficiency by 30%. Comparing the results obtained in the case of prototype number 2 with the retention efficiency of a classic cabin filter made of microfibers, one can notice a much higher overall efficiency of the classic filter. The major difference being made on the size range 0.33-0.85 μm, the ceramic filter obtaining better performances on the range 0.85-2.33 μm.
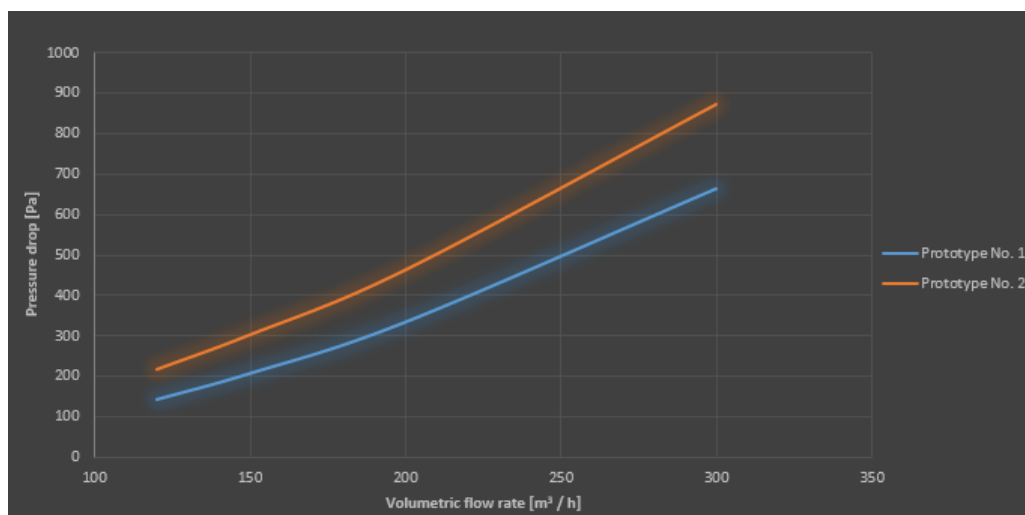
Figure 9. Pressure drop graph generated by the filter elements
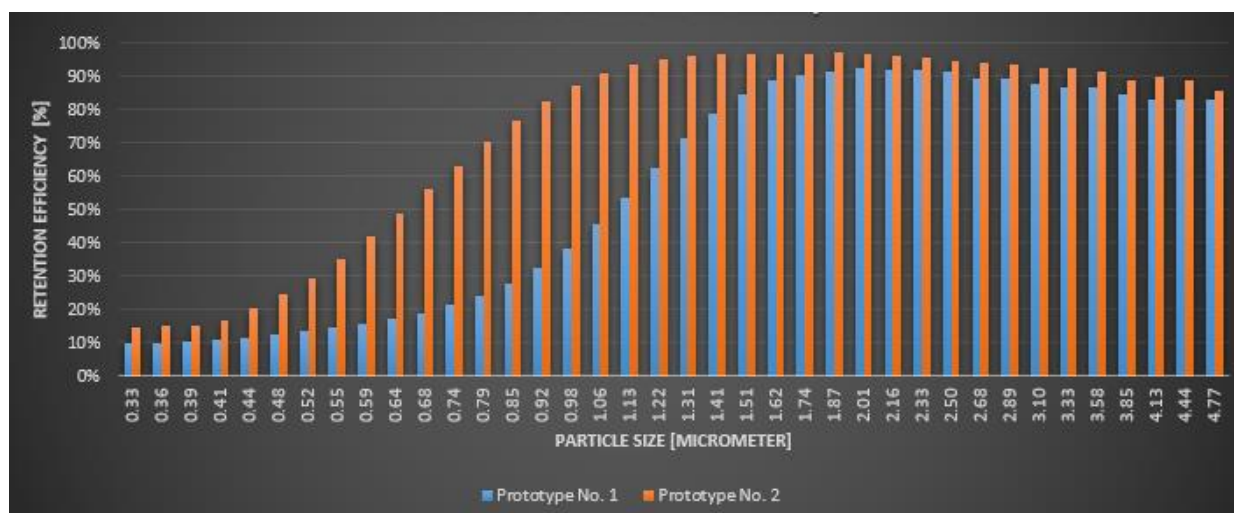
Figure 10. Particle retention efficiency
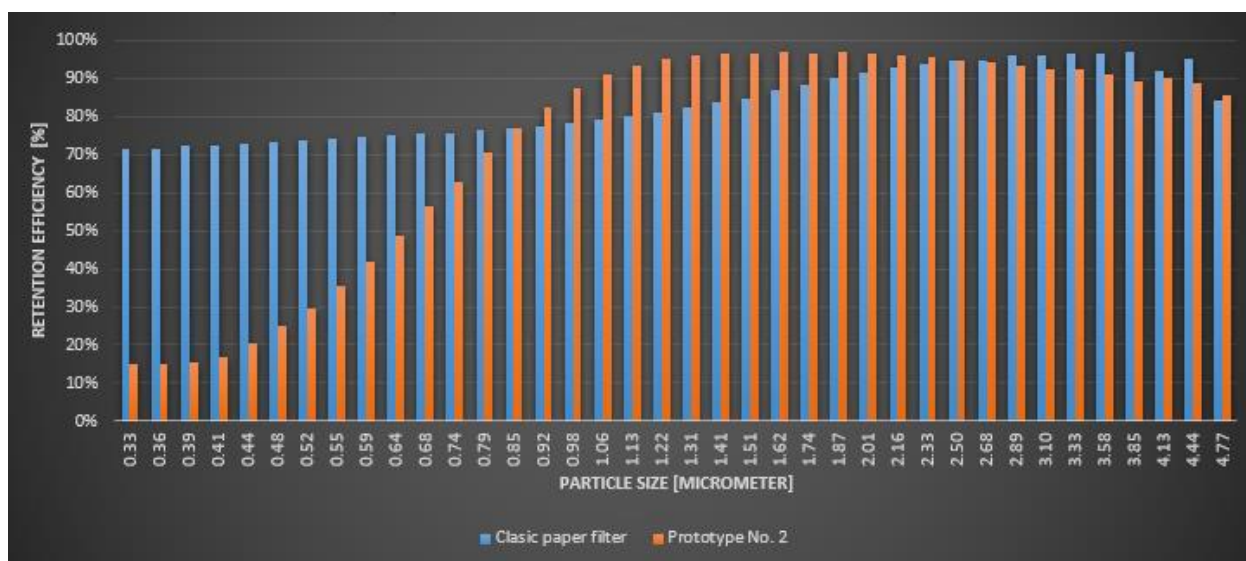
Figure 11. Comparison with a classic paper filter retention efficiency

5. CONCLUSION

Among the advantages offered using ceramic materials in gas filtration is their ability to retain gases at the molecular level. One of the most common processes in which porous ceramics are used to separate gases of different types is the pressure swing adsorption (PSA) process, this process being used to separate a particular species of gas from a gas mixture. Porous ceramic filter elements could be a viable alternative to conventional microfiber filters. Following the dissemination of the results obtained, it follows that the retention efficiency of porous ceramic filters could be improved by increasing the density of the filter element. Also, the retention capacity on specific size ranges can be correlated by density variation. In conclusion, the integration of ceramic materials in the process of air filtration in the form of a filter element could replace the classic filtration solutions and improve air quality by retaining harmful gaseous compounds.

REFERENCES

[1] Pujadó, P. R.; Rabó, J. A.; Antos, G. J.; Gembicki, *Industrial catalytic applications of molecular sieves.* S. A. (1992-03-11)

[2] Williams, D. B. G., Lawton, M., "*Drying of Organic Solvents, Quantitative Evaluation of the Efficiency of Several Desiccants",* The Journal of Organic Chemistry 2010, vol. 75, 8351

[3] Topas GMBH, *https://www.topas-gmbh.de/wordpress/dateien/produkte/112PAF_Cabin_AirFilter_TestSystem_Gas.pdf*

[4] Cruceanu, M. Popovici, E. Bâlba, N. Naum, N. Vlădescu, L. Russu, R. Vasile, A., *Site moleculare zeolitice.* Publisher: Editura Științifică Și Enciclopedică București 1986

[5] Birtok Băneasă C., *Research regarding the use of advanced materials for the optimization in the intake proecss of the internal combustion engines,* Politehnica University of Timisoara, Romania, Doctoral Thesis 2019

ASPECTS RELATED TO PROPULSION SYSTEM MODELING AND RESISTIVE FORCES FOR TRACKED VEHICLES

Octavian ALEXA[1)*], Iulian COROPEȚCHI[1)], Alexandru VASILE[1)], Andrei INDREȘ[1)], Laszlo BAROTHI[1)], Alexandru DOBRE[2)]

[1)] Military Technical Academy „FERDINAND I", Department of Military Automotive and Transportation, Bdul George Coşbuc, Nr. 39-49, 050141 BUCHAREST, Romania
[2)] University Politehnica of Bucharest, Department of Road Vehicles, Splaiul Independenței, Nr. 313, 060042 BUCHAREST, Romania

Abstract: *This paper describes the algorithm for calculating the power flow required to overcome the forward resistances of a tracked vehicle, which is equipped with a high-power diesel engine. The laws underlying the nodal theory were used to develop the model for simulating the longitudinal dynamics of the tracked vehicle: the law of conservation of energy and the law of equilibrium of load factors. Thus, the entire structure of the vehicle, including the propulsion system of the tracked vehicle, is identified by network nodes, each node being assigned the energy conservation conditions and the dependencies on the other nodes. The proposed model takes into account the differential analytical equations regarding the dynamics of the vehicle, the interaction with the roadway and its chassis. The modeling results highlight the power required to overcome the forward resistances, the time variation of the torque that loads the drive wheel of the vehicle and the performance of the vehicle when running on a horizontal terrain.*

NOMENCLATURE

F_{ja} - the load factor of the inertial power flow of the tracked robot
$\tilde{F}_p$, F_{pd} – dynamic propulsion force
f_{pr} – rolling resistance coefficient of the propulsion system
$\tilde{F}_t$, F_{td} – dynamic traction force
G_a – weight of the tracked robot
I_{pr} - moment of inertia of the propulsion system wheels
m_a – mass of the tracked vehicle.
M_{jpr} - the reduced torque at the drive wheel of the inertial forces of the propulsion system
M_{rd}, $\tilde{S}$ - the dynamic torque that actually loads the drive wheel after the acceleration of the masses in rotational motion
$\tilde{M}_{rm}$ – dynamic torque at the drive wheel
$M_{\mu fpr}$ - reduced torque at the drive wheel of the moments of friction in the propulsion system
R_aer, R_a – air resistance
R_alpha, R_α – slope resistance
R_sol, R_s – soil deformation resistance
R_{pr} – rolling resistance of the propulsion system
T - the dynamic tangential reaction with which the support branch of the track acts on the ground
UGV - Unmanned Ground Vehicle
ω_{rm} - angular speed of the drive wheel
v – speed of the vehicle
$P_{\tau pr}$ – power flow lost to overcome the rolling resistance force of the propeller
r_{rm} – sprocket radius

Corresponding author e-mail: octavian.alexa @mta.ro

1. INTRODUCTION

The tracked vehicle in this study is based on the chassis of a tank. The aim of this research is to develop a tracked vehicle that can move without being driven by a driver. We suggest the idea of developing an autonomous / semi-autonomous robotic platform on the structure of a tracked military vehicle. This transformation must allow intervention in emergency response missions [1][2][3]. The energy system, which delivers the necessary energy to the propulsion system, is an internal combustion engine [4][5].

The decision to study the possibility of transforming a military combat vehicle into an emergency robot was made based on the following challenges: climate change, terrorism, social crises, destruction of the forest area [6][7][8][9][10][11]. Each of them has different features, which viewed separately have a greater or lesser impact depending on the gradient of the respective states. The simultaneous occurrence of several risk situations can generate unpredictable effects, which can endanger the intervention staff. On the other hand, any of the challenges mentioned above can become causes of the occurrence of the others. One of the biggest problems is the disasters caused by fires that occur in the forest environment, in petrochemical plants or in areas of exploitation of oil fields [12][13]. Also, among the risks that require intervention with large robots are nuclear accidents, natural disasters, etc. The use of crawler intervention vehicles capable of autonomous / semi-autonomous intervention eliminates staff exposure. At the same time, they have an increased capacity to extinguish fires or limit the effects caused by various disasters [8][14]. One of the problems studied is the behavior of the crawler engine. The present study concerns, in particular, the power flow required to overcome the forward resistance of a tracked military vehicle.

This desideratum comes from the fact that for the development of a navigation system of a tracked terrestrial robot we must know how the variable parameters, from the relations that describe the kinematics and dynamics of the respective vehicle, influence the laws of movement.
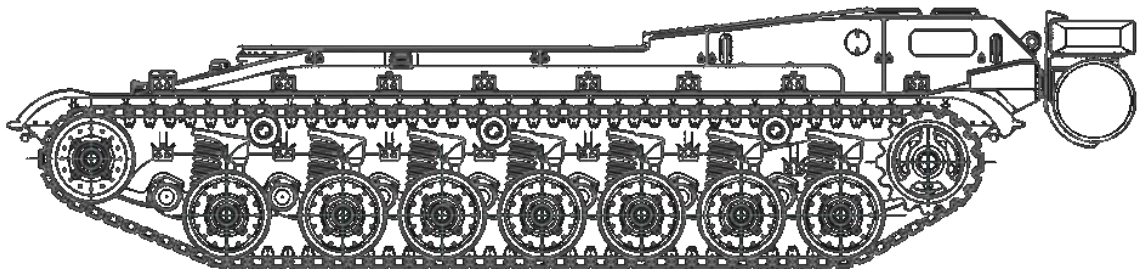
Figure 1 – Representation of the tracked propulsion system on a tank chassis

The general idea of the research is to develop a family of robots that will be able to intervene in multiple situations, just by replacing some components. In other words, the robotic system will consist of two subsystems:

- transport vector - chassis and engine;
- operational vector - intervention systems, which can be attached to the chassis.

By operational vectors we mean: crane, bulldozer blade, fire extinguishing system [15], tools specific to engineering activities, demining systems, etc. The operational vector will also be equipped with the following: command-control system, communication system, sensor system [1][4][5][7].

Until now, the studies carried out by the research staff of the Military Technical Academy "Ferdinand I" can be found in the works [1][3][4][8][16][17][18]. The present study considers the terrain undeformable. In reality, it is an unstructured work environment [16][17][19][20][21].

2. PROPULSION SYSTEM AND FORWARD RESISTANCE MODELING

The tracked propulsion system allows the transformation of the rotational mechanical power flow, characterized by torque and angular velocity, into the mechanical translational power flow, characterized by force and speed [6].

The power flow (Figure 2) of the propulsion system is influenced by the variation of load and kinematic factors, the moments of inertia of the components and the internal power losses caused by sliding and rolling friction [1][17].
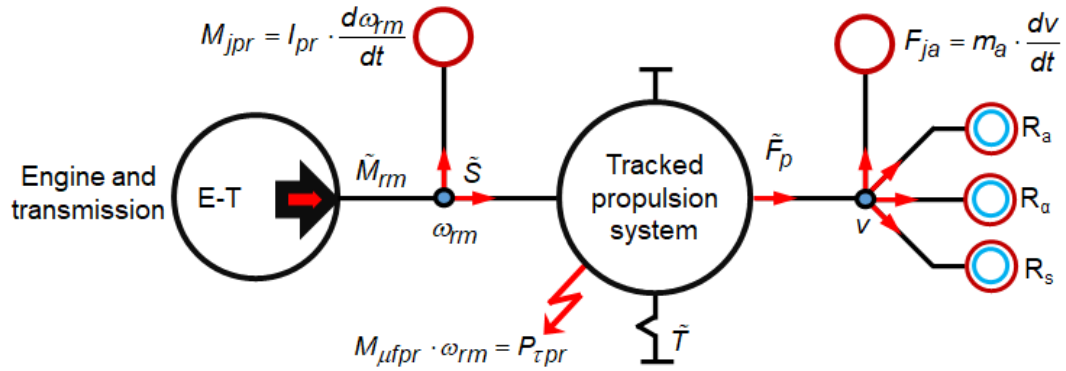
Figure 2 – Nodal representation of the forces and moments acting on the tracked propulsion system

The equations resulting from the application of the laws of load factors equilibrium and energy conservation factors [6,13] allow to determine the expression of the dynamic traction force of the tracked vehicle:

$$
\left.
\begin{aligned}
&\tilde{M}_{rm} - I_{pr} \cdot \frac{d\omega_{rm}}{dt} - \tilde{S} = 0 \qquad P_{\tau pr} = M_{\mu fpr} \cdot \omega_{rm} \\
&\tilde{S}\,\omega_{rm} - \tilde{F}_p v - P_{\tau pr} = 0 \qquad M_{\mu fpr} = R_{pr} \cdot r_{rm} \\
&\tilde{F}_p - F_{ja} - R_a - R_s - R_\alpha = 0 \quad \tilde{M}_{rm} = \tilde{F}_t \cdot r_{rm}
\end{aligned}
\right\}
\xrightarrow{v=\omega_{rm} r_{rm}}
\begin{aligned}
&\tilde{F}_p = F_{ja} + R_a + R_s + R_\alpha \\
&\tilde{F}_t = \tilde{F}_p + \left(\frac{I_{pr}}{r_{rm}^2}\right)\frac{dv}{dt} + R_{pr}
\end{aligned}
\tag{1}
$$

Next, for the modeling of the mentioned active and resistant factors we use the Simscape-Matlab programming language [18][22] and we implement in code form the differential algebraic equations generated from the energy conservation and equilibrium conditions of the load factors [5].
The blocks resulting from the modeling are grouped to simulate the dynamic operation of the tracked propulsion system (Figure 3).
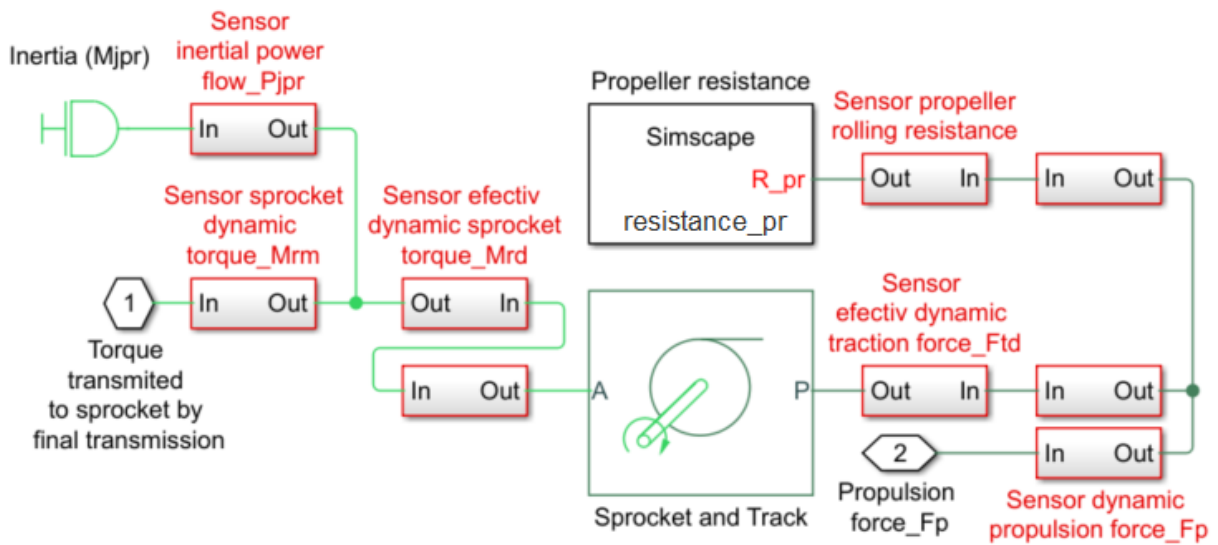
Figure 3 – Representation of the simulation of the propulsion system made in Simscape-Matlab

The modeling of the load factor of the inertial power flow Mjpr was performed with one of the predefined blocks in the library of the Simscape Multibody ™ Matlab module. In order to model the physical process of transforming the factors of the rotational motion field into the factors of the translational motion domain and the phenomenon generated by the rolling resistance force of the propulsion system, our own library was developed with the blocks "Sprocket and Track" and "resistance _ pr".

The source codes of the blocks that describe the two phenomena are based on the following equations:

$$M_{rd} = F_{td} \cdot r_{rm} \ [Nm] \tag{2}$$

$$v = \omega_{rm} \cdot r_{rm} \left[\frac{m}{s} \right] \tag{3}$$

$$R_{pr} = f_{pr} \cdot G_a \cdot \cos(\alpha) \ [N] \tag{4}$$

$$f_{pr}(v) = 3e^{-2} + 143e^{-2} \cdot 3,6 \left(v + 1,2e^{-6} \cdot 3,6v^2 \right) [-] \tag{5}$$

The sets of algebraic equations, added to the system of general equations describing the dynamic operation of the crawler vehicle, allow transformation of the factors of the two mechanical domains (rotation, translation), rolling resistance force modeling [16][17] and modeling of acceleration resistance [1]. Solving the system of equations, with the help of Matlab software, allows later visualization of physical signals [23][24], signals that represent the time variation of the dynamic torque received by the drive wheel from the final transmission (M_{rm}) (Figure 4), the load factor of the inertial power flow consumed to accelerate the rotating masses (M_{jpr}) (Figure 5), the dynamic moment that actually loads the drive wheel after the acceleration of the masses in rotational motion (M_{rd}) (Figure 6), dynamic traction force (F_{td}) (Figure 7), the rolling resistance force of the propulsion system (R_{pr}) (Figure 8) and dynamic propulsion force (F_{pd}) (Figure 9).

From the interpretation of the graphs the following can be noticed:
- the rolling force of the propeller increases with increasing the speed;
- the load factor of the inertial power flow consumed to accelerate the masses in rotational motion decreases with increasing the speed.
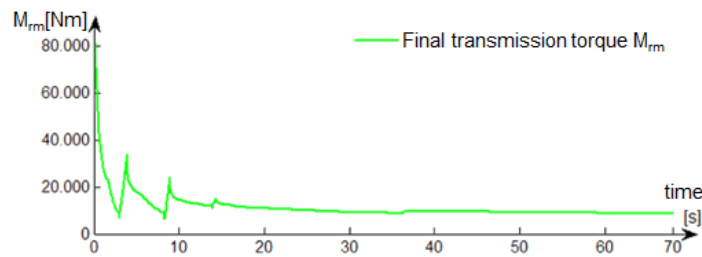
Figure 4. Variation of the dynamic torque received by the drive wheel from the final transmission (Mrm)
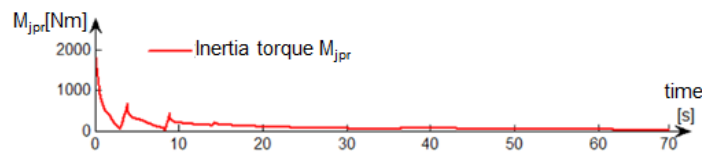
Figure 5. Variation of the load factor of the inertial power flow consumed to accelerate the masses in rotating motion (Mjpr)
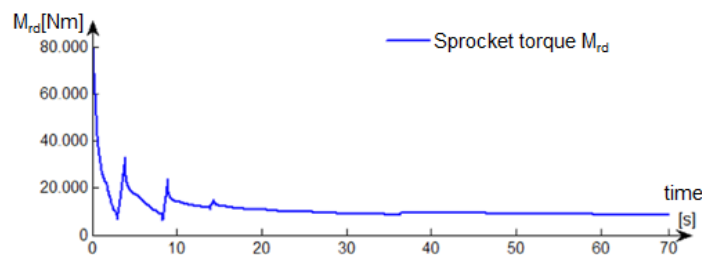
Figure 6. Variation of the dynamic moment that actually loads the drive wheel after the acceleration of the masses in the rotational motion (Mrd)
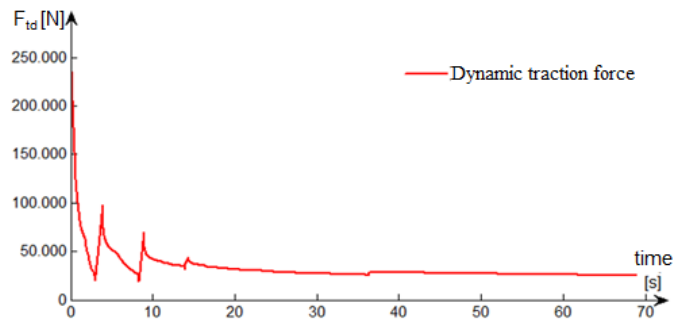
Figure 7. Variation of dynamic traction force (Ftd)
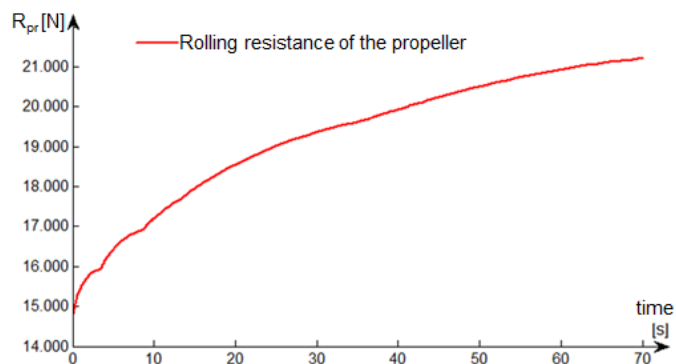
Figure 8. Variation of the rolling resistance force of the propulsion system (Rpr)
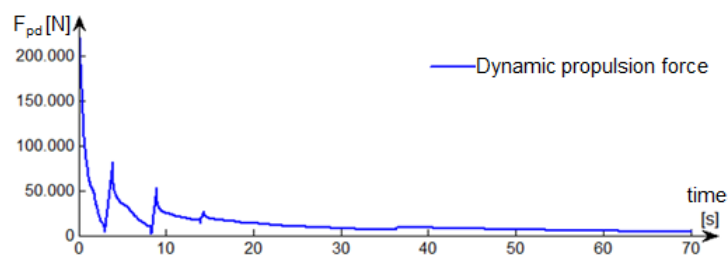
Figure 9. Variation of dynamic propulsion force (Fpd)
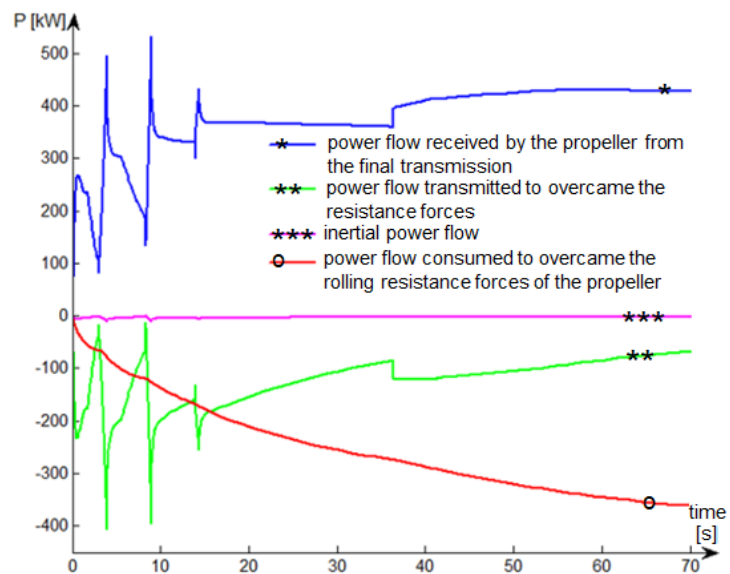
Figure 10 - Energy balance of the tracked propulsion system

Following the calculations performed (1 ÷ 5) results the graph in Figure 10, in which it is presented:

- the energy balance received by the engine;
- the balance of energy consumed in the form of dissipative and inertial flow;
- the balance of energy transmitted to overcome forward resistance.

The dynamic propulsion force is equal to the sum of all the resisting forces acting on the tracked vehicle, represented by: air resistance (R_aer), slope resistance (R_alpha), resistance due to soil deformation (R_sol) and part of the acceleration resistance, due to the action of the inertial force generated by the acceleration Force_inertia [16][19].

The highlighting of these power losses is represented in the Simscape programming environment by the blocks of approximation of the resistance forces [17].
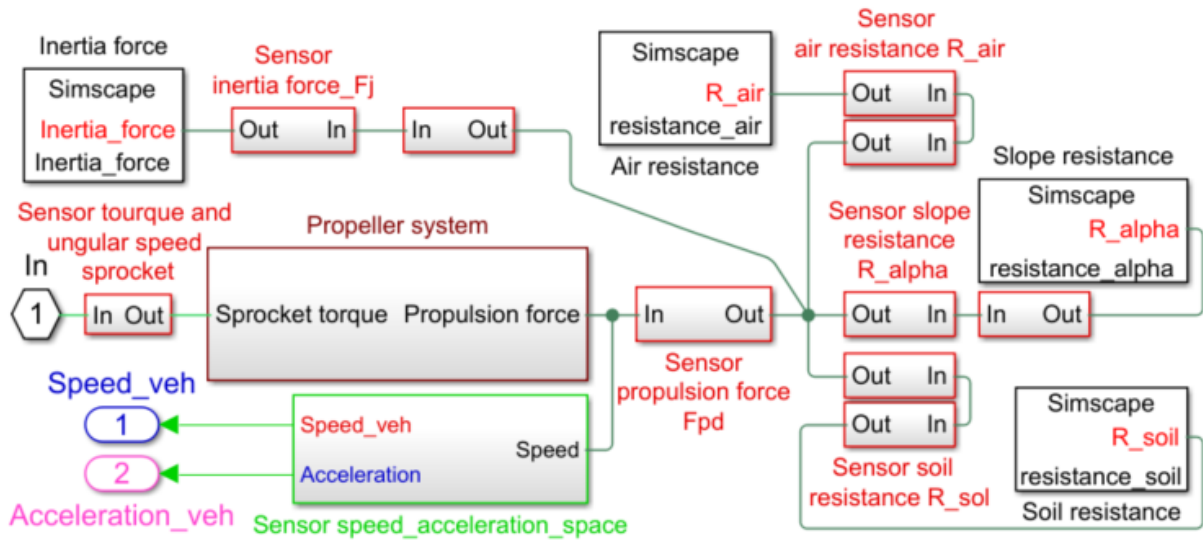

Figure 11 – Soil_propulsion_vehicle component

Subsequently, by attaching the blocks within the "soil_propulsion_vehicle" component, the model for simulating the interaction between the road, propulsion system and chassis is completed (Figure 11). In the modelling diagram of the component "Soil_propulsion_vehicle" the block "sensor_speed_acceleration_space" appears (Figure 12).

The block is used to take from the energy network the signals specific to the UGV's travel speed, acceleration and the space travelled by it during the simulation (Figure 13).

The final simulation model (Figure 14) [1][16][17] is built for the main systems of the tracked vehicle.

The blocks of the general longitudinal dynamic's simulation model have defined physical connection ports, which are used as connectors [17].
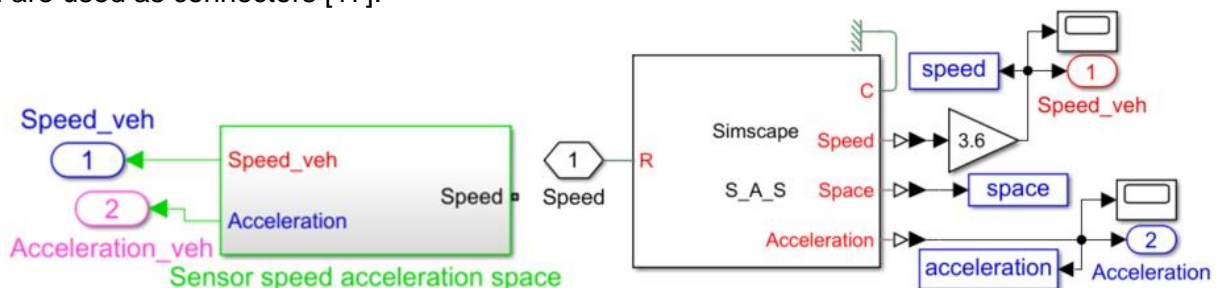
Figure 12 – Sensor speed_acceleration_space component

When programming the simulation model (Figure 14) the following simplifying hypotheses were established: the engine always runs at its maximum load, the terrain on which the engine runs is hard and flat, and the movement of the vehicle is linear and accelerated.

To validate the general simulation model, the simulation results were compared with those obtained experimentally [16][17].

The rectilinear displacement experiment was performed under the following conditions: the position of the accelerator pedal was depressed until the end of the stroke and was maintained in this position throughout the experimental test, and the gear change was performed according to the specifications set by the manufacturer [25].
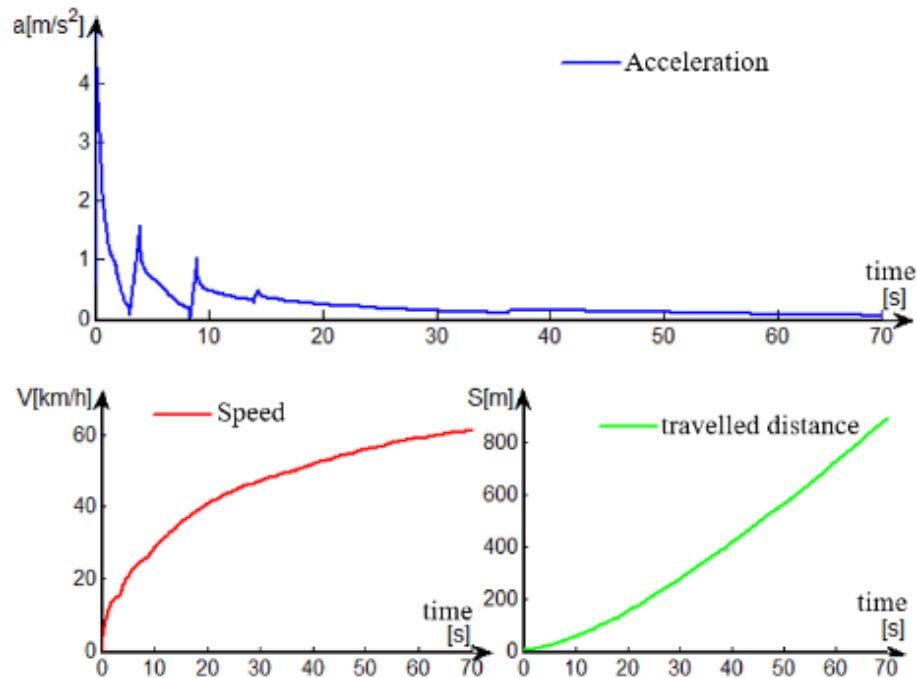
Figure 13 - Variation of acceleration, speed and space as a function of time
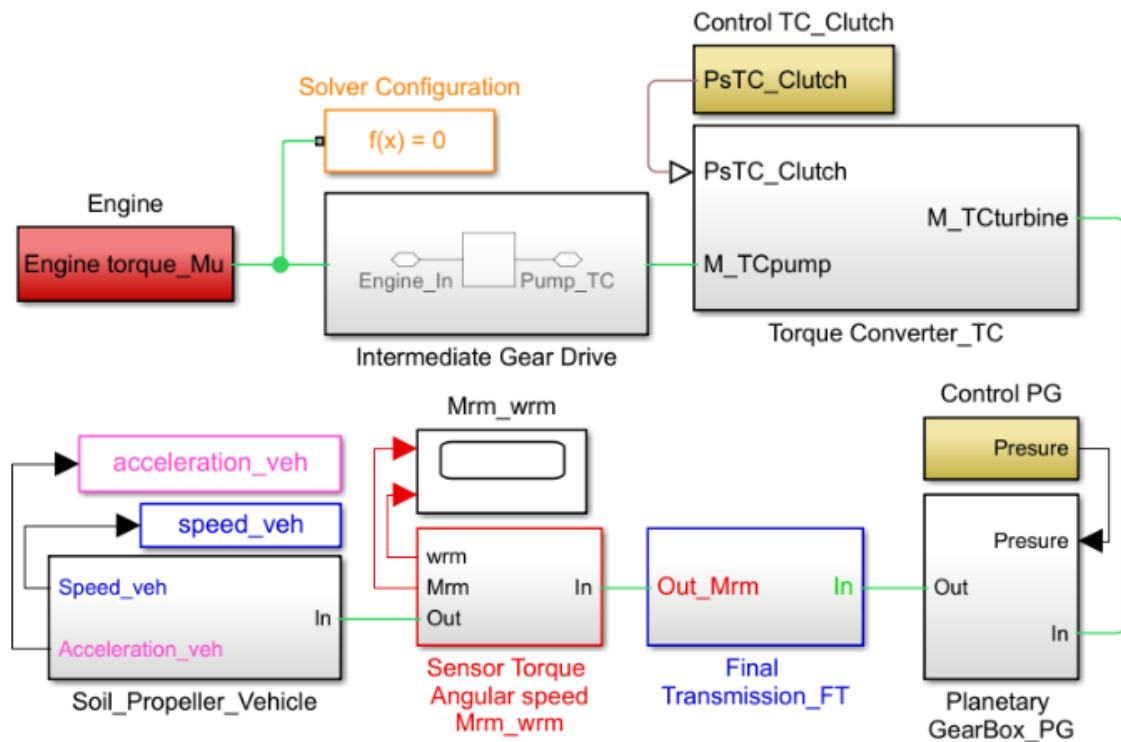
Figure 14 - General simulation model of the tracked vehicle
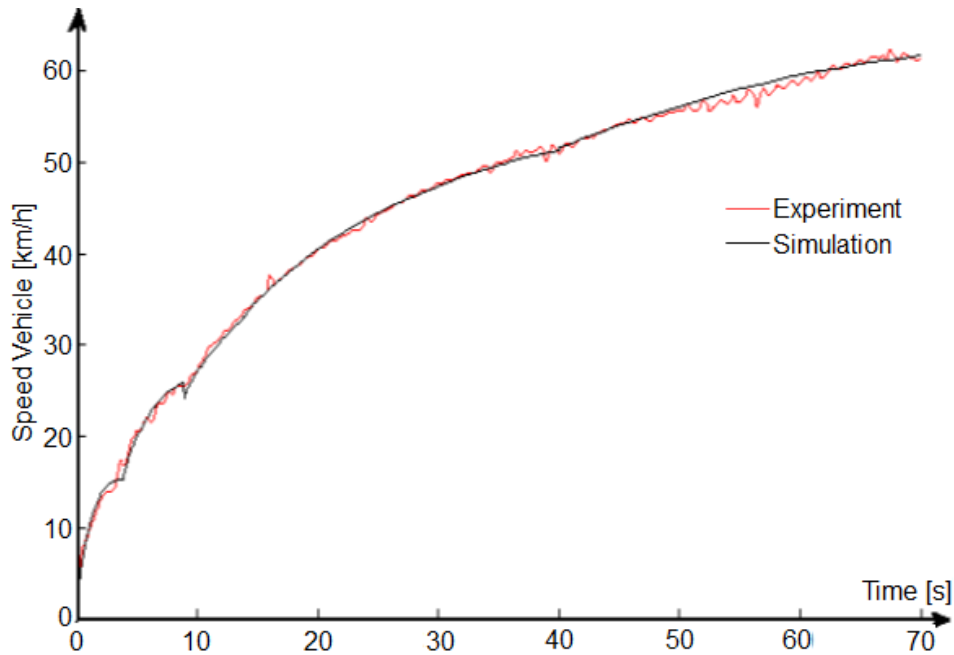
Figure 15 - Validation of the general simulation model

In Figure 15 we can see the graphs of the two types of determining the speed of the tracked vehicle, respectively by simulation and experiment. It can be seen that the graph of the speed obtained by simulation overlaps in a very good ratio over the graph obtained experimentally.

3. CONCLUSIONS

Following the tests performed on the performances of the tracked propulsion system at rectilinear movement, it was found that the analytical model proposed for the calculation of the kinematics and dynamics elements is a valid model.
The information is based on the fact that the error, from the data obtained by simulation differs from those obtained experimentally, is below the threshold of 6% (Figure 15).
This encourages us to continue our research in order to transform the tracked vehicle, driven by a driver mechanic, into a semi-autonomous crawler robot for emergency response.
We provide the following arguments in support of these affirmations:
- the algorithm consists of modules programmed in the Simscape language, which contain the equations they describe:
  - tracked vehicle kinematics;
  - tracked vehicle dynamics;
  - estimation of torque and angular velocity at the inputs and outputs of each component;
  - acceleration pedal position;
- determining the required power because the conditions of progression are met according to the forward resistance;
- determining the variation of the dynamic torque at the drive wheel;
- determining the variation of the power flow to accelerate the masses in rotating motion.

We believe that the proposed goal of developing an analytical model that describes how forward resistances influence the dynamics of the tracked propulsion system engine is achieved.
Next, we will design the hardware and software elements to transform the tracked vehicle into a special purpose robot.

5. REFERENCES

[1] Alexa, O.; Coropețchi, I.; Vasile, A.; Oncioiu, I. and Grigore, L.Ș., *Considerations for Determining the Coefficient of Inertia Masses for a Tracked Vehicle*. MDPI, Sensors, vol. 20, issue 19, pag. 1-34, 2020.

[2] Grigore, L.Ș.; Soloi, A.; Tiron, O. and Răcuciu, C., *Fundamentals of autonomous robot classes with a system of stabilization of the gripping mechanism*. Advanced Materials Research, vol. 646, pag. 164-170, 2013.

[3] Nuță, I.; Orban, O. and Grigore, L.Ș., *Development and improvement of technology in emergency response*. Procedia Economics and Finance, vol. 32, pp. 603-609, 2015.

[4] Ciobotaru, T. and Grigore, L.Ș, *Robot pentru combaterea acțiunilor teroriste ROBTER,* Proiect de cercetare CEEX-2006, Aria tematică 9.1, Protecția împotriva terorismului și a crimei. Platforma tehnologică PT4 - Advanced engineering materials and technologies, Academia Tehnică Militară, București.

[5] Stoica, P.M. and Molder, C., *Comparative analysis of methods to detect radio-controlled commercial UAVs*. 4th International Scientific Conference SEA-CONF, Scientific Bulletin of Naval Academy 2018, Vol. XXI 2018, pag.45-49, 2018.

[6] Costinas, S.; Otomega, B., Cherecheș, T., Sava, A.C. and Ioniță, E, *Management of emergency situations resulting from technological hazard, natural catastrophes and terrorist attacks*. World scientific and engineering academy and society, vol. Proceedings of the 11th WSEAS International conference on sustainability in science engineering, pag. 320 – 324, 2009.

[7] Grigore, L.Ș.; Priescu, I. and Grecu, D.L., *Inteligența Artificială Aplicată în Sisteme Robotizate Fixe și Mobile.* Editura AGIR. Bucharest. 2020.

[8] Grigore, L.Ș.; Priescu, I; Joița, D. and Holban-Oncioiu, I., *The Integration of Collaborative Robot Systems and Their Environmental Impacts*, MDPI, Processes, vol. 8, issue 4, pag. 1 - 11, 2020.

[9] Grigore, L.Ș.; Ileri, R.; Neculăescu, C.; Soloi, A.; Ciobotaru, T. and Vînturiș, V, *A Class of autonomous robots prepared for unfriendly sunny environment*, Informatics in Control, Automation and Robotics. Lecture Notes in Electrical Engineering, vol. 132, issue 1, pag. 73-80, 2011.

[10] HONG, D., Virginia Tech takes on Department of Defense challenge to build disaster-response robots, http://www.vtnews.vt.edu/articles/2012/10/102412-engineering-thorrobotannouncement.html, 2012.

[11] Insurance Information Institute. Loss events worldwide 1980 – 2014. NatCatSERVICE, Geo Risks Research, Munich: Münchener Rückversicherungs-Gesellschaft, 2015.

[12] Petrochemical incidents.HM Fire Service Inspectorate Publications Section London: The Stationery Office, https://www.ukfrs.com/sites/default/files/2017-9/Fire_Service_Manual_Volume 2_Fire_Service_ Operations-Petrochemical Incidents 0.pdf

[13] Priddy, D.J., *Stochastic Vehicle Mobility Forecasts using NATO Reference Mobility Model*, *Technical Report GL-95-8*, US Army Corps of Engineers, Waterways Experiment Station, 1995.

[14] Tan, C.F.; Liew, S.M.; Alkahari, M.R.;. Ranjit, S.S.S; Said, M.R.; Chen, W.; Rauterberg, G.W.M. and Malingam, S.D., *Fire Fighting Mobile Robot: State of the Art and Recent Development*. Australian Journal of Basic and Applied Sciences, vol. 7(10), pag. 220-230, 2013.

[15] Ciobotaru, T., Grigore, L.Ș, Vînturiș, V.M., Grosu, D., *Mașina de Intervenție la sonde – MIS-PETROM 01 – Efectuarea de măsurători, verificări și determinări conform planului de testare-evaluare a produsului*, Ministerul Apărării Naționale, PSCD, nr. 1981, 1998.

[16] Alexa, O.; Vilău, R.; Ilie, O.C.; Voicu, D. and Marinescu, M., *Aspects regarding the kinematic optimization of a tracked military vehicle's transmission*. CONAT 2016 International congress of automotive and transport engineering, vol. 1, pag. 348-353, Springer International Publishing, 2017.

[17] Alexa, O., Truță, M.; Marinescu, M.; Vilău, R. and Vînturiș, V, *Simulating the longitudinal dynamics of a tracked vehicle*, Advanced Materials Research, vol. 1036, pp. 499-504, 2014.

[18] Truță, M; Fieraru (Alexa), O.; Vilău, R.; Vînturiș, V. and Marinescu, M., *Static and dynamic analysis of a planetary gearbox working process*. Advanced Materials Research, vol. 837, pag. 489 – 494, 2014.

[19] Ciobotaru, T. and Alexa, O., *Ingineria Autovehiculelor Militare cu Șenile. Vol. III: Transmisia. Frânele. Agregatul Energetic*. Publishing House of the Military Technical Academy "Ferdinand I". Bucharest. 2019.

[20] Ilie, C.O.; Marinescu, M.; Alexa, O.; Vilău, R. and Grosu, D., *Statistical models of petrol engines vehicles dynamics*. IOP Conference Series: Materials Science and Engineering, Vol. 252, issue 1, 2017.

[21] Nuță, I.; Grigore, L.Ș.; Orban, O.; Vînturiș, V. and Ciobotaru, T., *Aspects on the Mobility Electric Propulsion of Wheeled Robotic Platform.* 4th International conference on materials engineering for advanced technologies, pag. 623-626, 2015.

[22] Stefan, A.; Constantin, D. and Grigore, L.Ș., *Aspects of kinematics and dynamics of a gripping mechanism*. Proceedings of the 7th International conference on Electronics, computers and artificial intelligence (ECAI), pag. WF1 – WF4, 2015.

[23] Marinescu, M. and Ilie. C.O., *Filtering the signal of a measured mechanical parameter*. Institute of Electrical and Electronics Engineers, 10th International Conference on Communications, pag. 1 – 4, 2014.

[24] Ilie, C.O.; Marinescu, M.; Alexa, O.; Voicu, D. and Barothi, L., *Correlation analysis - a data analysis tool in the vehicle dynamics modeling process*. Romanian Journal of Automotive Engineering, issue 44, pag. 9 – 12, 2017.

[25] Test bulletin for the Experimental Research Laboratory for Armored Vehicles, Automobiles and Tractors - LACEBAT, within the Military Technical Academy „FERDINAND I".

AIMS AND SCOPE

The Romanian Journal of Automotive Engineering has as its main objective the publication and dissemination of original research in all fields of „Automotive Technology, Science and Engineering". It fosters thus the exchange of ideas among researchers in different parts of the world and also among researchers who emphasize different aspects regarding the basis and applications of the field.

Standing as it does at the cross-roads of Physics, Chemistry, Mechanics, Engineering Design and Materials Sciences, automotive engineering is experiencing considerable growth as a result of recent technological advances. The Romanian Journal of Automotive Engineering, by providing an international medium of communication, is encouraging this growth and is encompassing all aspects of the field from thermal engineering, flow analysis, structural analysis, modal analysis, control, vehicular electronics, mechatronics, electro-mechanical engineering, optimum design methods, ITS, and recycling. Interest extends from the basic science to technology applications with analytical, experimental and numerical studies.

The emphasis is placed on contribution that appears to be of permanent interest to research workers and engineers in the field. If furthering knowledge in the area of principal concern of the Journal, papers of primary interest to the innovative disciplines of „Automotive Technology, Science and Engineering" may be published.
No length limitations for contributions are set, but only concisely written papers are published. Brief articles are considered on the basis of technical merit. Discussions of previously published papers are welcome.

Notes for contributors
Authors should submit an electronic file of their contribution to the **Production office:** www. siar.ro. All the papers will be reviewed and assessed by a series of independent referees.

Copyright
A copyright transfer form will be send to the author. All authors must sign the "Transfer of Copyright" agreement before the article can be published.

Upon acceptance of an article by the journal, the author(s) will be asked to transfer copyright of the article to the publisher. The transfer will ensure the widest possible dissemination of information. This Journal and the individual contributions contained in it are protected by the copyright of the SIAR, and the following terms and conditions apply to their use:

Photocopying
Single Photocopies of single articles may be made for personal use as allowed by international copyright laws. Permission of the publisher and payment of a fee is required for all other photocopying including multiple or systematic copying, copying for institutions that wish to make photocopies for non-profit educational classroom use.

Derivative Works
Subscribers may reproduce table of contents or prepare lists of article including abstracts for internal circulation within their institutions. Permission of the publisher is required for resale or distribution outside the institution.
Permission of publisher is required for all other derivative works, including compilations and translations.

Electronic Storage
Permission of the publisher is required to store electronically and material contained in this journal, including any article or part of article. Contact the publisher at the address indicated.
Except as outlined above, no part of this publication may be reproduced, stored in a retrieval system or transmitted in any form or by any means, electronic, mechanical, photocopying, recording or otherwise, without prior written permission of the publisher.

Notice
No responsibility is assumed by the publisher for any injury and or damage to persons or property as a matter of products liability; negligence or otherwise, or from any use or operation of any methods, products, instructions or ideas contained in the material herein. Although all advertising material is expected to conform to ethical (medical) standards, inclusion in this publication does not constitute a guarantee or endorsement of the quality or value of such product or of the claims made of it by its manufacturer.

The Scientific Journal of SIAR
A Short History

The engineering of vehicles represents the engine of the global development of the economy.

SIAR tracks the progress of the automotive engineering in Romania by: the development of automotive engineering, the development of technologies, and road transport services; supporting the work of the haulers, supporting the technical inspection and of the garage; encouraging young people to have a career in the automotive engineering and road haulage; stimulation and coordination of activities that promote an environment that is suitable for continuous education and improving of knowledge of the engineers; active exchange of ideas and experience, in particular for students, master students, PhD students, and young engineers, and dissemination of knowledge in the field of automotive engineering; cooperation with other technical and scientific organizations, employers' and socio-professional associations through organization of joint actions, of mutual interest.

By the accession to FISITA (International Federation of Automotive Engineering Societies) since its establishment, SIAR has been involved in achieving an overall professional community that is homogeneous in competence and performance, interactive, dynamic, and competitive at the same time, oriented towards a balanced and friendly relationship between people and the environment; this action will be constituted as a challenge worthy of effort and recognition.

The insurance of a favorable framework for the initiation and the development of cooperation of the specialists in this field of activity allows for an efficient and easy exchange of information, specific knowledge and experience; it supports the cooperation between universities and between research centers and industry; it speeds up the process of implementing the new technologies, it simplifies the identification of training and specialization needs of the personnel involved in the engineering of motor vehicles, transport, and road safety.

In order to succeed, ever since its founding, SIAR has considered that the stress should be put on the production and distribution, at national and international level, of a publication of scientific quality.

Under these circumstances, the development of the scientific magazine of SIAR had the following evolution:

1. RIA – Revista inginerilor de automobile (in English: ***Journal of Automotive Engineers***)
ISSN 1222 – 5142

Period of publication: 1990 – 2000	Format: print, Romanian
Frequency: Quarterly	Electronic publication on: www.ro-jae.ro
Total number of issues: 30	Type: Open Access

The above constitutes series nr. 1 of SIAR scientific magazine.

2. Ingineria automobilului (in English: ***Automotive Engineering***)
ISSN 1842 – 4074

Period of publication: as of 2006	Format: print and online, Romanian
Frequency: Quarterly	Electronic publication on: www.ingineria-automobilului.ro
Total number of issues: 60	Type: Open Access

(Including the September 2021 issue)
The above constitutes series nr. 2 of SIAR scientific magazine (Romanian version).

3. Ingineria automobilului (in English: ***Automotive Engineering***)
ISSN 2284 – 5690

Period of publication: 2011 – 2014	Format: online, English
Frequency: Quarterly	Electronic publication on: www.ingineria-automobilului.ro
Total number of issues: 16	Type: Open Access

(Including the December 2014 issue)
The above constitutes series nr. 3 of SIAR scientific magazine (English version).

4. *Romanian Journal of Automotive Engineering*
ISSN 2457 – 5275

Period of publication: from 2015	Format: online, English
Frequency: Quarterly	Electronic publication on: www.ro-jae.ro
Total number of issues: 27 (September 2021)	Type: Open Access

The above constitutes series nr. 4 of SIAR scientific magazine (English version).

Summary

Total of series:	*4*
Total years of publication:	*27 (11: 1990 – 2000; 16: 2006 – 2021)*
Publication frequency:	*Quarterly*
Total issues published:	*90 (Romanian), out of which, the last 43 were also published in English*